Volatile organic compounds composition of merged and aged forest fire plumes from Alaska and western Canada

J. A. de Gouw,[1,2] C. Warneke,[1,2] A. Stohl,[1,2,3] A. G. Wollny,[1,2] C. A. Brock,[1,2] O. R. Cooper,[1,2] J. S. Holloway,[1,2] M. Trainer,[1] F. C. Fehsenfeld,[1] E. L. Atlas,[4] S. G. Donnelly,[5] V. Stroud,[6] and A. Lueb[6]

Received 3 May 2005; revised 1 December 2005; accepted 13 January 2006; published 23 May 2006.

[1] The NOAA WP-3 aircraft intercepted aged forest fire plumes from Alaska and western Canada during several flights of the NEAQS-ITCT 2k4 mission in 2004. Measurements of acetonitrile (CH_3CN) indicated that the air masses had been influenced by biomass burning. The locations of the plume intercepts were well described using emissions estimates and calculations with the transport model FLEXPART. The best description of the data was generally obtained when FLEXPART injected the forest fire emissions to high altitudes in the model. The observed plumes were generally drier than the surrounding air masses at the same altitude, suggesting that the fire plumes had been processed by clouds and that moisture had been removed by precipitation. Different degrees of photochemical processing of the plumes were determined from the measurements of aromatic VOCs. The removal of aromatic VOCs was slow considering the transport times estimated from the FLEXPART model. This suggests that the average OH levels were low during the transport, which may be explained by the low humidity and high concentrations of carbon monoxide and other pollutants. In contrast with previous work, no strong secondary production of acetone, methanol and acetic acid is inferred from the measurements. A clear case of removal of submicron particle volume and acetic acid due to precipitation scavenging was observed.

Citation: de Gouw, J. A., et al. (2006), Volatile organic compounds composition of merged and aged forest fire plumes from Alaska and western Canada, *J. Geophys. Res.*, *111*, D10303, doi:10.1029/2005JD006175.

1. Introduction

[2] Forest fires, and biomass burning in general, are large sources of reactive trace gases in the atmosphere. For example, approximately 25% of carbon monoxide (CO) and nitrogen oxides (NO_x) emissions to the global atmosphere are from biomass burning [*Brasseur et al.*, 1999]. These estimates and the impact of the emissions on the atmosphere are quite uncertain, however, because of the fact that reliable data on biomass burning are much more sparse than data on anthropogenic sources. Unlike anthropogenic pollution, the location and timing of forest fires are hard to predict, which makes it difficult to study the emissions, their transport and chemical transformation in a concerted effort.

[3] The emissions of volatile organic compounds (VOCs) from biomass burning and the VOC chemistry in fire plumes are relatively uncertain. Numerous emissions measurements have been performed in the laboratory [e.g., *Lobert et al.*, 1990; *Yokelson et al.*, 1996; *Holzinger et al.*, 1999; *Schauer et al.*, 2001; *Christian et al.*, 2003, 2004], and there are a number of field studies. For example, Yokelson and coworkers have characterized VOCs in smoke plumes over Alaska, North Carolina and Africa [*Yokelson et al.*, 1999, 2003; *Goode et al.*, 2000; *Sinha et al.*, 2003], and *Friedli et al.* [2001] collected air samples in a number of North American forest fire plumes and analyzed these for VOCs. Fewer papers have described the chemical processes involving VOCs within forest fire plumes. *Hobbs et al.* [2003] described the rapid removal of VOCs in an African fire plume. *Yokelson et al.* [2003] observed the removal of methanol from a cloud-processed smoke plume in Africa, and *Tabazadeh et al.* [2004] suggested an explanation for the chemical mechanism. *Jost et al.* [2003] made airborne measurements at several distances downwind from an agricultural fire in Namibia, and observed secondary formation of acetone within two hours after emission. *Holzinger et al.* [2005] observed relatively high methanol and acetone enhancements in fire plumes over the Mediterranean and concluded that secondary production of these species must have taken place. Finally,

[1]NOAA Aeronomy Laboratory, Boulder, Colorado, USA.
[2]Also at Cooperative Institute for Research in Environmental Sciences, University of Colorado, Boulder, Colorado, USA.
[3]Now at Norwegian Institute for Air Research, Kjeller, Norway.
[4]Rosenstiel School of Marine and Atmospheric Science, University of Miami, Miami, Florida, USA.
[5]Department of Chemistry, Fort Hays State University, Hays, Kansas, USA.
[6]National Center for Atmospheric Research, Boulder, Colorado, USA.

Copyright 2006 by the American Geophysical Union.
0148-0227/06/2005JD006175$09.00

several authors observed secondary formation of acetic acid in smoke plumes from forest and savanna fires [*Goode et al.*, 2000; *Hobbs et al.*, 2003; *Yokelson et al.*, 2003; *Trentmann et al.*, 2005]. In general, the photochemistry in fire plumes is active, and formation of ozone was reported in numerous studies [*Wofsy et al.*, 1992; *Mauzerall et al.*, 1996; *Goode et al.*, 2000; *McKeen et al.*, 2002].

[4] In July and August of 2004 a large-scale atmospheric chemistry and transport study was conducted over North America and Europe within the framework of the ICARTT collaboration (International Consortium for Atmospheric Research on Transport and Transformation). As part of the NOAA contribution to ICARTT, the NEAQS-ITCT 2k4 (New England Air Quality Study–Intercontinental Transport and Chemical Transformation) study was conducted, which involved airborne measurements using the NOAA WP-3 research aircraft based out of Portsmouth, New Hampshire. During the NEAQS-ITCT 2k4 study period extensive forest fires were burning in Alaska and western Canada. Smoke from the forest fires was observed over the continental United States in satellite images from GOES (Geostationary Operational Environmental Satellites), and the MOPITT (Measurements of Pollution in the Troposphere) and AIRS (Atmospheric Infrared Sounder) satellite instruments observed extensive plumes of CO [*Pfister et al.*, 2005]. Emissions from forest fires in Alaska and Canada have the potential to impact regional air quality in the United States [*Wotawa and Trainer*, 2000; *McKeen et al.*, 2002; *DeBell et al.*, 2004], and the ICARTT study provides a unique data set to study the chemical processes during the transport in detail.

[5] The NOAA WP-3 sampled plumes from the Alaskan and western Canadian fires on multiple flights after transport times ranging from a few days to two weeks. Using measurements of acetonitrile (CH_3CN), an indicator of biomass burning [*de Gouw et al.*, 2003a], and the atmospheric transport model FLEXPART, these air masses were unambiguously attributed to forest fires in Alaska and western Canada. In this paper, the VOC composition of the fire plumes is described. The removal of the emitted trace gases by chemical reactions and precipitation is studied, as is the secondary formation of oxygenated VOCs within the fire plumes. Subsequent papers will focus on the observations of ozone, nitrogen species and particles in the fire plumes.

2. Airborne Measurements

2.1. Aircraft Measurements

[6] A total of 18 flights were made between 5 July and 15 August 2004, using a NOAA WP-3 aircraft based in Portsmouth, New Hampshire. Flight objectives included the characterization of emissions from cities in the eastern United States (e.g., New York City and Boston), point sources (e.g., power plants in Ohio), and forest vegetation. The roles of transport, mixing and chemical transformation were studied in polluted air masses. Additional measurements were performed during the transfer flights between Tampa, Florida, and Portsmouth on 5 July and 15 August 2004. The extensive instrumental payload of the NOAA WP-3 allowed a detailed characterization of the chemical and aerosol composition of the atmosphere. A full description of the payload is beyond the scope of this paper and will be presented in subsequent papers on the NEAQS-ITCT 2k4 experiment.

2.2. PTR-MS Measurements

[7] Airborne measurements of methanol (CH_3OH), acetonitrile (CH_3CN), acetaldehyde (CH_3CHO), acetone (CH_3COCH_3), acetic acid (CH_3COOH), methyl ethyl ketone (MEK; $C_2H_5COCH_3$), aromatic VOCs (benzene, toluene, C_8- and C_9-aromatics) and several other compounds (dimethyl sulfide, isoprene, methyl vinyl ketone, methacrolein and monoterpenes) were made with a proton-transfer-reaction mass spectrometer (PTR-MS; Ionicon Analytik) [*de Gouw et al.*, 2003b]. PTR-MS measurements of these species have been validated by a ship-based comparison with an online GC-MS instrument [*de Gouw et al.*, 2003c], and possible interferences have been studied by *Christian et al.* [2004] and by combining PTR-MS with a gas chromatographic preseparation method [*de Gouw et al.*, 2003a, 2003b; *Warneke et al.*, 2003]. The reader is referred to these references for a detailed description of the PTR-MS used in this work. Only the details pertinent to the present paper are given below.

[8] The response of the PTR-MS was calibrated between flights using a standard mixture of seven VOCs (methanol, acetonitrile, acetaldehyde, dimethyl sulfide, acetone, benzene and toluene) in nitrogen. The sensitivities for the other VOCs used in this work were determined using standard mixtures before and after the NEAQS-ITCT 2k4 mission. For most of these species the calibration accuracy is estimated to be better than 15%, except for methanol, the C_9-aromatics and the monoterpenes. The response for methanol is difficult to calibrate because of memory effects in the pressure regulator and flow controller that are used with the standard gas mixture [*de Gouw et al.*, 2003c], and the calibration accuracy is estimated to be 25%. For the C_9-aromatics and the monoterpenes, the PTR-MS measurement determines the summed mixing ratio of multiple species: two propyl benzene, three trimethyl benzene and three ethyl toluene isomers in case of the C_9-aromatics, and α- and β-pinene, camphene, myrcene, α-limonene, 3-carene and several other species in case of the monoterpenes [*de Gouw et al.*, 2003c]. The instrument was calibrated for all these compounds separately, and the resulting accuracy of the averaged calibration was estimated to be 25%.

[9] We have not developed a reliable calibration standard for acetic acid. During the New England Air Quality Study in 2002, the PTR-MS response at 61 amu correlated well with acetic acid measurements by ion chromatographic analysis of mist chamber samples [*de Gouw et al.*, 2003c]. From the comparison the sensitivity for acetic acid was estimated to be 8.0 counts s^{-1} $ppbv^{-1}$, normalized to an H_3O^+ count rate of 10^6 counts s^{-1} (ncps $ppbv^{-1}$). Using the same sensitivity for the NEAQS-ITCT 2k4 data gave much higher mixing ratios in similar conditions. It is suspected that the ship measurements in 2002 suffered from losses of acetic acid inside the long inlet line that was used with the PTR-MS. As a result the estimated sensitivity was a factor of 4–8 lower than for other VOCs. In the aircraft measurements a much shorter inlet was used, which probably limited the inlet losses, and also gave a much improved response time for measurements at 61 amu. In this work, we

Table 1. Calibrated Sensitivities of the PTR-MS Measurements Used in This Work, the Comparison With the WAS Measurements, and the Estimate of Measurement Precision

Compound	Sensitivity, ncps ppbv^{-1}	r	Slope	Intercept, pptv	Background, counts s^{-1}	Scatter, pptv	
						Measured	Calculated
Methanol	26.8				870		160
Acetonitrile	50.7				17		12
Acetaldehyde	55.8				600		63
Acetone	63.8				310		39
Acetic acid	41.4				800		98
MEK	70.0	0.87	0.85 ± 0.02	57 ± 4	320	58 ± 3	37
Benzene	31.4	0.87	1.08 ± 0.02	12.8 ± 1.4	35	25.6 ± 0.6	27
Toluene	39.8	0.90	0.88 ± 0.02	4.3 ± 1.5	36	30.2 ± 1.2	22
C_8-aromatics	54.9	0.91	0.856 ± 0.013	−0.5 ± 0.5	33	16.3 ± 0.2	15
C_9-aromatics	44.0	0.79	1.03 ± 0.03	24.6 ± 0.6	26	17.12 ± 0.12	17

have estimated the sensitivity for acetic acid using a calculation that involves the reaction time of H_3O^+ ions in the drift tube, and the rate coefficient for the reaction between H_3O^+ and acetic acid [*de Gouw et al.*, 2003b]. Such calculated sensitivities have been shown to be accurate within 50% [*Warneke et al.*, 2003]. Inlet losses were not quantified during the NEAQS-ITCT 2k4 mission and the acetic acid data should be regarded as approximate. In addition, *Christian et al.* [2004] have shown that glycolaldehyde can contribute to the signal at 61 amu in fresh fire emissions.

[10] The sensitivities for all VOCs are summarized in Table 1. For many of the species the sensitivities are within 5% of the published values from NEAQS 2002 [*de Gouw et al.*, 2003c]. Calibrations with newly obtained standard mixtures were performed for acetaldehyde, MEK and the C_8-aromatics, for which the comparison with the GC-MS measurements during NEAQS 2002 revealed some calibration inaccuracies. The measurement precision of PTR-MS is limited by the background signals due to impurities in the system, and can be calculated from the Poisson counting statistics of the ion signals [*de Gouw et al.*, 2003c]. The background signals and the calculated precision of the PTR-MS measurements, using the average observed H_3O^+ signal of 8×10^6 counts s^{-1}, are also shown in Table 1.

[11] During the NEAQS-ITCT 2k4 mission, the PTR-MS monitored a total of 16 masses attributed to different VOCs, and 4 additional masses for the primary (H_3O^+, $H_3O^+.H_2O$) and impurity (NO^+, O_2^+) ions from the ion source. The measurement time per VOC mass was 1 s, and the total measurement cycle took about 17 s. The background levels of VOCs in the instrument were determined every 30 cycles (~10 min) by passing the sample flow through a Pt catalyst heated to 350°C.

2.3. Analyses of the Whole Air Samples

[12] During every flight, up to 80 whole air samples (WAS) were collected in electropolished stainless steel gas canisters. The time to fill a canister varied between 5 and 25 s. The canisters were transported to the NCAR laboratory in Boulder, where they were analyzed within a few days for hydrocarbons and halocarbons using several gas chromatography (GC) techniques. *Schauffler et al.* [1999, 2003, and references therein] describe the methods of sampling and analysis. Because of sampling problems no data are available for the flights on 5, 9 and 11 July. Only a small number of canisters were actually collected in fire plumes, and the results of the WAS measurements are used in this paper for comparison with the PTR-MS data: the aromatic VOCs (benzene, toluene, C_8- and C_9-aromatics) and MEK were measured by both instruments, in case of the WAS with a 10% uncertainty [*Ryerson et al.*, 2003].

2.4. Comparison Between the PTR-MS and WAS Data

[13] Of the VOCs used in this work, the aromatics and MEK were quantified by both the PTR-MS and the WAS. Measurements of dimethyl sulfide, isoprene, methyl vinyl ketone, methacrolein and monoterpenes were also performed by both PTR-MS and WAS. However, these VOCs were not detected in the forest fire plumes, and the generally good agreement between the measurements will be discussed elsewhere. The PTR-MS and WAS results for the aromatics and MEK from the entire mission are compared in Figures 1a, 1c, 1e, 1g, and 1i. The fill times of the WAS instrument were in many cases shorter than the cycle time of the PTR-MS, and thus only a fraction of canister measurements coincided perfectly with a PTR-MS data point. For the purpose of this comparison, the PTR-MS data were linearly interpolated onto the midpoints of the WAS sampling periods. The linear correlation coefficient between the PTR-MS and WAS data, r, ranged from 0.79 for the C_9-aromatics to 0.91 for the C_8-aromatics. The solid lines in Figure 1 show the results of one-sided, least squares linear fits to the data. The slopes and intercepts from the fits are shown in Table 1, and all slopes are equal to one within the calibration accuracy of 15%. We also tried to calculate two-sided regressions to the data, which minimize the orthogonal distance between the data and fit instead of the vertical distance [*Bakwin et al.*, 1997; *de Gouw et al.*, 2003c]. However, the calculation of two-sided regressions did not converge to accurate results for the slopes, probably because the majority of the data points were at the lower range of the measured mixing ratios. Only few samples were collected in fire plumes, and the data did not diverge from the general trends observed in Figure 1. In the WAS data for MEK, there were several outliers that were not observed by the PTR-MS, and were also not present as outliers in the CO data. These data points are indicated by the solid black circles in Figure 1a, and have not been included in the fit. The WAS data did not include n-propyl benzene, but this compound can contribute to the PTR-MS signal that is attributed to C_9-aromatics. n-Propyl benzene typically encompasses about 7% of the total emissions of C_9-aromatics [*de Gouw et al.*, 2005]. If this compound had been included, the slope between PTR-MS and WAS would most likely still be equal to one within 15%. It should be noted

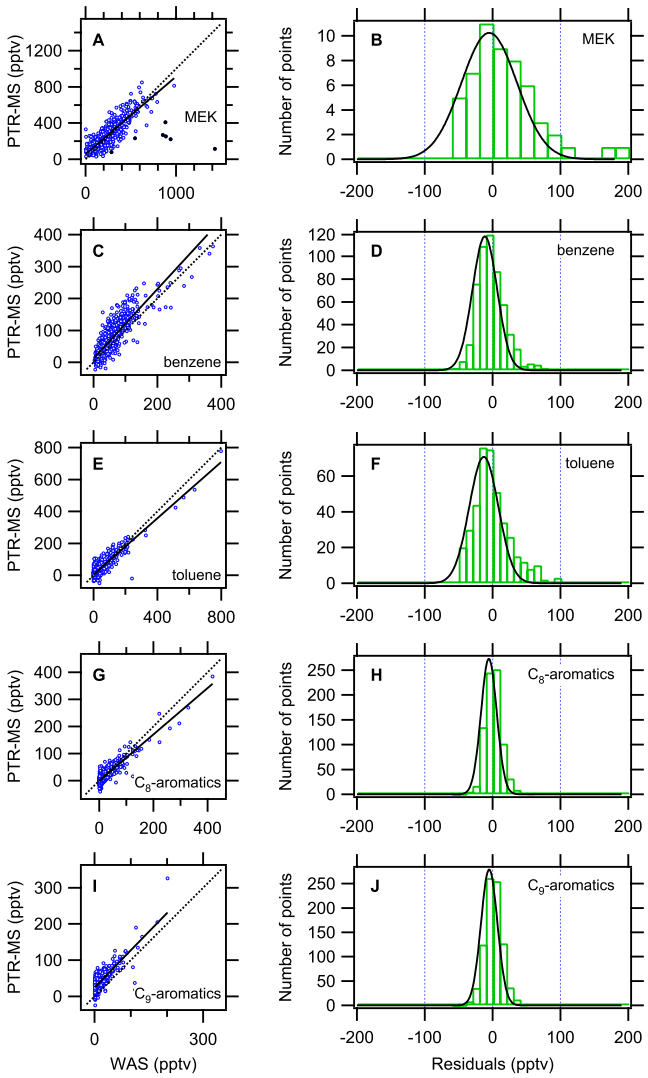

Figure 1. Comparison between the PTR-MS and WAS measurements. The plots on the left show all data with the solid lines the results of linear fits and the dotted lines the 1:1 line. The plots on the right show the distribution of residuals from the linear fits for all points below 50 pptv in the left plots. Included are the results for (a and b) MEK, (c and d) benzene, (e and f) toluene, (g and h) C_8-aromatics and (i and j) C_9-aromatics.

that the standards used to calibrate the WAS and PTR-MS measurements were not compared for this experiment.

[14] Figures 1b, 1d, 1f, 1h, and 1j show the distribution of the residuals between data and linear fits, in order to quantify the amount of scatter in the PTR-MS measurements. The distribution is limited to those data points below 50 pptv: the scatter increases with mixing ratio, whereas at the lowest mixing ratios the scatter is mostly determined by the background signals and can be calculated from the sensitivity and those background signals [*de Gouw et al.*, 2003c]. The solid curves give the results of fits of a Gaussian function to these distributions, and the widths from those fits (1σ) are given in Table 1. The scatter in the data is the highest for MEK, the lowest for the C_8-aromatics, and can be compared with the calculated scatter given in Table 1. For benzene and the C_8- and C_9-aromatics the scatter in the measurements agrees well with the calculated scatter, whereas for toluene and MEK the scatter in the measurements is somewhat higher than calculated. In the case of MEK, the difference between measured and calculated scatter may be due to the fact that the background signal is humidity-dependent: the $H_3O^+(H_2O)_3$ water cluster ion is also detected at 73 amu. In the case of toluene the difference may be due to impurities in the inlet line; unlike previous missions, the PTR-MS measurements suffered from occasional signal bursts at 93 amu, particularly during ascents. These artifacts have been removed from the data.

[15] In conclusion, the WAS and PTR-MS agreed quantitatively for MEK, benzene, toluene and the C_8- and C_9-aromatics. For MEK and the C_8-aromatics this is an improvement over the results from NEAQS 2002, when the disagreement between PTR-MS and GC-MS was outside the estimated measurement accuracies. In addition, the remaining differences between the WAS and PTR-MS measurements of benzene and the C_8- and C_9-aromatics can be quantitatively explained by the limited counting statistics of the PTR-MS measurement.

2.5. Carbon Monoxide Measurements

[16] Carbon monoxide (CO) was determined using a vacuum ultraviolet fluorescence measurement as described by *Holloway et al.* [2000]. The precision of the measurements is estimated to be 2.5%. Variability in the determination of zero levels results in an absolute uncertainty of about 1 ppbv in the values reported. The field standard was compared to NIST Standard Reference Material (SRM) 2612a (10 ppmv nominal CO in air). We estimate that the concentration of our calibration standard is known to within 2%. The overall accuracy of the 1 s measurements is thus estimated to be 5%.

2.6. Particle Volume Measurements

[17] Aerosol particle volume was calculated from size distributions measured with a 1 s time response using three instruments that together span the particle diameter range from 0.003 to 8.2 μm. The instruments were as described by *Brock et al.* [2004], except that particles with diameters from 0.6 to 8.2 μm were measured with a custom-built optical particle counter that used a white light-emitting diode as the light source. The accuracy of the particle volume measurement is limited primarily by uncertainty in the refractive index of the particles, which is unknown for the smoke particles. Calibrations of the particle sizing instruments were made using particles with three different refractive indices. Propagation of the response of the instruments through the data processing algorithms produce accuracy and precision estimates of ±40% and ±10%, respectively. The volumes reported are for dry (<40% relative humidity) conditions; they are not corrected for ambient humidity.

3. Results and Discussion

3.1. North American Forest Fires in 2004

[18] In the summer of 2004, extensive forest fires were burning in Alaska and western Canada. Figure 2 shows maps of the estimated CO emissions. In late June 2004, just before the NEAQS-ITCT 2k4 mission started, the fires were

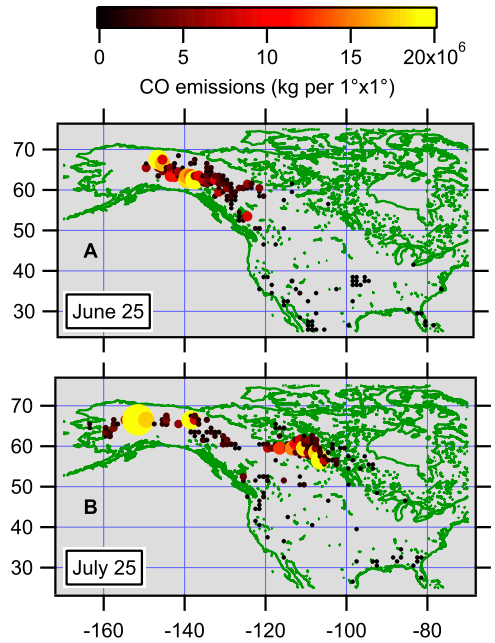

Figure 2. Location of the forest fires in Alaska and western Canada (a) on 25 June, just before the NEAQS-ITCT 2k4 mission started, and (b) on 25 July, when there were forest fires closer to the study area in the eastern United States.

mostly located in Alaska and western Canada (Figure 2a), whereas in late July 2004, later on during the mission, there were also fires further East (Figure 2b). The daily areas burnt per political province were taken from a webpage at the Center for International Disaster Information (http://www.cidi.org/wildfire) and smoothed with a 3-day running mean. Actual fire locations were determined using the number of fire hot spots detected by the MODIS instruments onboard the Aqua and Terra satellites. The hot spots were counted daily on a 1 × 1 degree grid and for every 3-day period the maximum daily number of hot spots was taken in order to account for possibly missing detections during cloudy periods. The areas burned in the provinces were then attributed to the grid cells by weighting with the number of hot spots. Finally, a constant emission factor of 4.5×10^5 kg CO per km^2 burned was used to obtain daily CO emission fields. This emission factor is consistent with emission measurements from crown fires performed in the Canadian Northwest Territories [*Cofer et al.*, 1998], which should be comparable to the 2004 fires in Alaska and western Canada, and was confirmed by previous long-range transport model calculations [*Wotawa and Trainer*, 2000; *Forster et al.*, 2001].

3.2. Aircraft Measurements of Forest Fire Plumes

[19] Emissions from the Alaskan and Canadian fires were sampled on a total of eight flights of the NOAA WP-3 research aircraft. The tracks of those eight flights are shown in Figure 3, color-coded by the measured mixing ratio of acetonitrile (CH_3CN), a sensitive tracer for biomass burning [*de Gouw et al.*, 2003a]. Fire plumes were observed over eastern Canada on 9 and 28 July (Figures 3a and 3h), over New England on 11, 20–22 and 25 July (Figures 3b and 3d–3g), and south of Cape Cod on 15 July (Figure 3c). During two of those flights the fire plumes were also observed in the continental boundary layer: around Boston on 11 July and in eastern Canada on 28 July. The highest mixing ratios of acetonitrile were measured on 9 July, whereas much lower mixing ratios were observed during the flights on 15 and 25 July. Smoke from the fires could often be seen in visible images from the GOES-EAST satellite at 1 km resolution. These images were used prior and during flights of the NOAA WP-3 to adjust the flight track and intercept the smoke plumes. It should be noted that other flight objectives, such as the study of regional air pollution, limited the time available to study forest fire plumes.

[20] We recently reported on the use of acetonitrile as an indicator of forest fire emissions over the North American continent [*de Gouw et al.*, 2003a]. It was shown that (1) acetonitrile was strongly enhanced in a forest fire plume over Utah that was sampled 2 hours downwind of the source, but (2) acetonitrile was not noticeably enhanced over the Los Angeles basin even though the levels of anthropogenic pollutants were very high. Similar observations were made during the NEAQS-ITCT study in 2004. Figure 4 shows scatterplots of acetonitrile versus CO for all flights shown in Figure 3. Some of the scatterplots contain two distinctively different groups of points, such as on 15, 20, 21 and 25 July (Figures 4c–4e and 4g). The data points with enhanced CO only were obtained in the outflow from nearby urban areas (New York City on 15 and 20 July, Boston on 21 July, Philadelphia on 25 July). The data points with both enhanced acetonitrile and CO were obtained in the forest fire plumes. It is interesting to note that the mixing ratios of CO measured in the urban and forest fire plumes were similar on 20 and 21 July, even though the urban outflow was measured tens of kilometers downwind and the fire outflow thousands of kilometers downwind from their respective sources. Acetonitrile and CO were well correlated during the entire flight on 9, 11 and 28 July, in which case the CO enhancements are solely attributed to forest fire emissions. The solid lines in Figure 4 show the results of linear fits to the data for the main forest fire plume intercepts, indicated by the shaded points in Figure 4, which are analyzed in detail further below. On some flights, for example on 25 July, acetonitrile was also enhanced elsewhere, but those plumes were harder to analyze because of the presence of nearby urban pollution plumes. The slopes from the fits in Figure 4 are shown in Table 2, and ranged from 1.18 pptv of acetonitrile per ppbv of CO on 15 July to 3.3 pptv $ppbv^{-1}$ on 22 July. These values are in the range of values reported in the literature (Table 2).

[21] Small but nonzero enhancements of acetonitrile were observed in some urban plumes. For example, the acetonitrile enhancement in the outflow from New York City on 20 July (Figure 4d) was found to be 0.25 ± 0.04 pptv $ppbv^{-1}$, which is higher than the enhancement of <0.1 pptv $ppbv^{-1}$ found for Los Angeles [*de Gouw et al.*, 2003a]. During other flights the measured acetonitrile enhancement in urban plumes was close to zero; the origin of observed small enhancements of acetonitrile in urban air remains unknown. A nonzero fraction of urban emissions may be due to the burning of biofuels (wood fires, barbecues, etc.). Despite the small urban acetonitrile enhancements, it is clear from

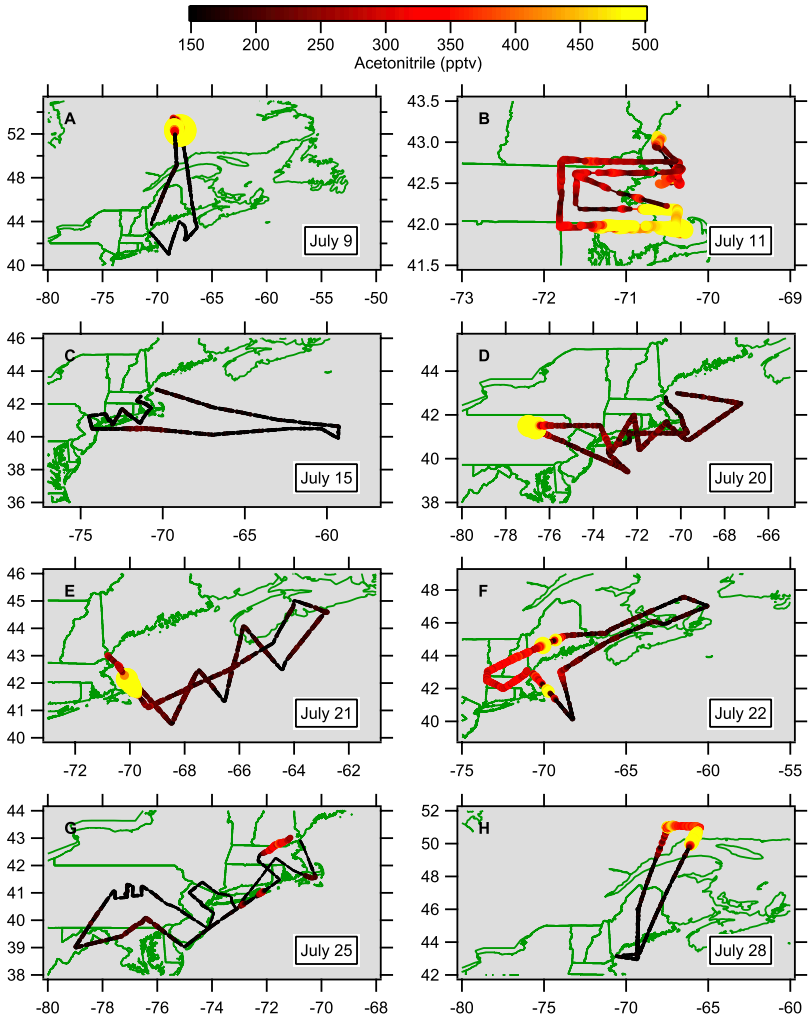

Figure 3. Flight tracks of the NOAA WP-3 on (a) 9 July, (b) 11 July, (c) 15 July, (d) 20 July, (e) 21 July, (f) 22 July, (g) 25 July and (h) 28 July, on which days the aircraft sampled forest fire plumes. The tracks are color-coded by the measured acetonitrile mixing ratios.

Figure 4 that this compound can be used as a sensitive indicator of forest fire emissions over North America.

3.3. Description of the Emissions Transport by FLEXPART

[22] The FLEXPART model was used to describe the transport of the emissions from the North American forest fires in 2004. FLEXPART is a Lagrangian particle dispersion model used to describe the long-range transport of pollutants in the atmosphere [*Stohl et al.*, 1998]. FLEXPART was run both forward and backward in time, but only the output from the backward runs was used here (see *Stohl et al.* [2003] for a description). For the backward runs, small boxes were created along the flight track and in every box, 40000 particles were released and tracked for 20 days backward in time. The model output, which has a global resolution of $1^\circ \times 1^\circ$ and 1 day, consists of a response function to emission input (i.e., an emission sensitivity), which is proportional to the residence time of the particles in a given volume. If multiplied with the gridded emission fluxes from the fire emission inventory and integrated over the volume of the atmosphere or parts of it, a mixing ratio at the aircraft location is obtained. In addition, the age spectrum of the mixing ratio obtained is known, i.e., the contributions from different transport times between emission and measurement. More information about the backward runs and results for all the flights can be found at the Website http://niwot.al.noaa.gov:8088/icartt_analysis/. For the location and emissions of the North American fires the FLEXPART model used the method outlined above in section 3.1.

[23] The transport was described in FLEXPART using meteorological data from both the ECMWF (European Center for Medium-Range Weather Forecasts), and the GFS (Global Forecast System) model of the National Center for Environmental Prediction (NCEP). The emissions of forest fires were evenly distributed over an altitude range of 0–1 km, 0–3 km and 0–10 km, respectively, to mimic the rapid vertical transport in fire-induced convective clouds that can be associated with large-scale forest fires [*Lavoué et al.*, 2000]. The FLEXPART model thus produced six different sets of output (ECMWF and GFS wind fields, three injection heights for each), and these will be compared with the results from the aircraft measurements in the following.

[24] Figure 5 shows the time series of the acetonitrile measurements from all flights that sampled forest fires,

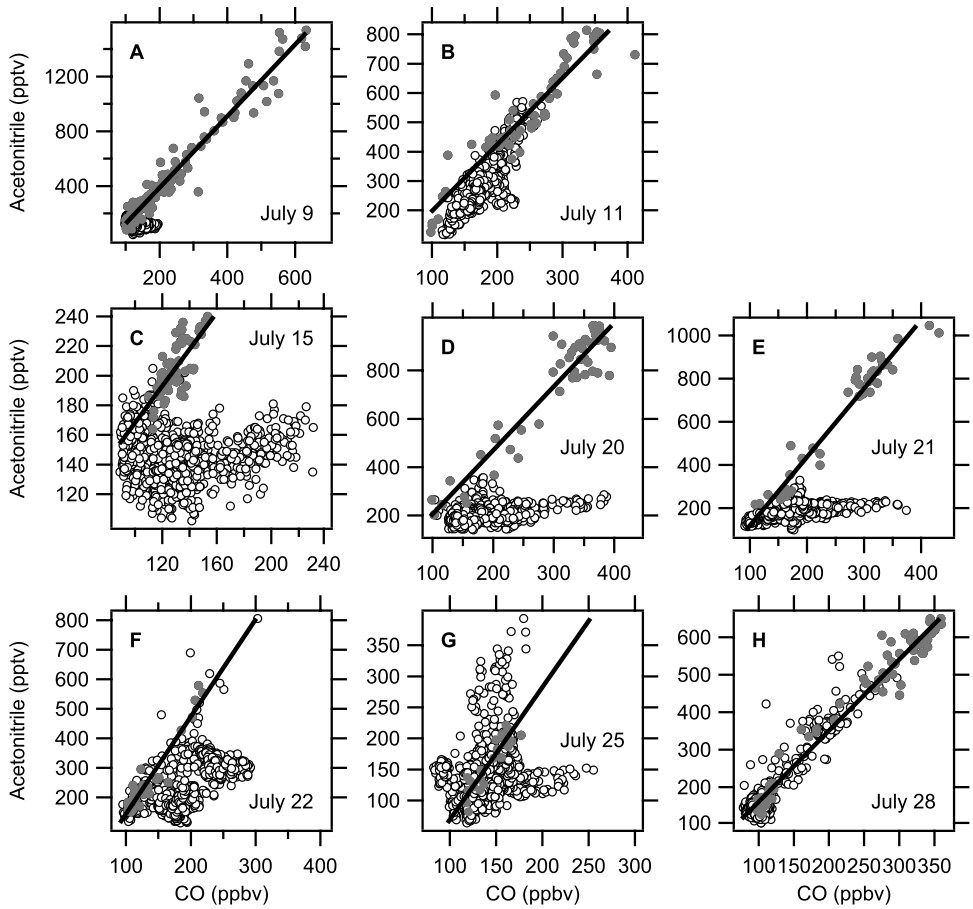

Figure 4. Scatterplots of acetonitrile versus CO for (a) 9 July, (b) 11 July, (c) 15 July, (d) 20 July, (e) 21 July, (f) 22 July, (g) 25 July and (h) 28 July. The open circles show the measured data from the entire flight, and the shaded circles show the data collected during the main fire plume intercepts. The solid lines show linear fits to the data measured during those intercepts.

along with the results from the FLEXPART model calculated along the flight track. In most cases the 0–1 and 0–3 km injection heights gave very similar results, and the 0–1 km injection height results have been omitted from Figure 5. For the purpose of these plots, the CO calculated with FLEXPART was converted to an acetonitrile mixing ratio using an acetonitrile emission ratio versus CO of 2.0 pptv ppbv^{-1}, and an acetonitrile mixing ratio of 120 pptv in the background troposphere [*de Gouw et al.*, 2003a]. In general, the FLEXPART model reproduced the location of the fire plumes very well. The best description was in most cases obtained using the ECMWF meteorological data and the 0–10 km injection heights. The FLEXPART model output generally underestimated the measured acetonitrile. A discussion for each flight follows:

[25] 1. On 9 July a fire plume was intercepted at 4 km altitude over eastern Canada. Both the ECMWF and GFS models reproduced the position of the fire plume on 9 July very well (Figure 5a). The 0–3 km and 0–10 km injection heights both gave similar results, but both underpredicted the observations.

[26] 2. On 11 July, fire emissions were observed both in a layer at 3 km and spread out over the boundary layer southeast of Boston. Only the GFS model described the layer at 3 km, and even gave a good quantitative description of the plume (Figure 5b). Only the ECMWF model reproduced the boundary layer observations, although it underpredicted the observations. For both the 3 km layer and the boundary layer observations, the 0–3 km injection heights gave a better description than the 0–10 km injection heights.

[27] 3. Both the GFS and ECMWF models captured the weak acetonitrile enhancement at 5 km on 15 July, but only using a 0–10 km injection height. The quantitative agreement between the ECMWF model, with the 0–10 km injection height, and the measurements is very good.

[28] 4. The ECMWF model described the layers at 3 km on 20, 21 and 22 July slightly better than the GFS model. Interestingly, a 0–10 km injection height had to be used to reproduce the layer at 3 km observed on 20 and 21 July: the model output for a 0–3 km injection height did not reproduce this layer. The model output for 20 and 21 July is a factor of 3–4 lower than the observations, whereas the quantitative agreement is good for 22 July. Also, the aircraft did not observe all of the features described by FLEXPART, for example the large peak around 1820 UTC on 21 July. In these cases the 0–3 km reproduced the data better. Figures 5d–5f show the ECMWF model with 0–3 and 0–10 km injection heights.

[29] 5. The ECMWF model with a 0–10 km injection height was the only model that described a weak acetonitrile enhancement early on in the flight of 25 July. Three stronger acetonitrile enhancements late in the 25 July flight were

Table 2. Enhancement Ratios Relative to CO Determined for Acetonitrile and Four Aromatic VOCs for the Different Forest Fire Plumes Sampled During NEAQS-ITCT 2k4

			Enhancement Ratios, pptv ppbv^{-1}				
Date	Start, UTC	Stop, UTC	Acetonitrile	Benzene	Toluene	C_8-Aromatics	C_9-Aromatics
9 July	2006	2057	2.55 ± 0.05	1.41 ± 0.04	0.44 ± 0.02	0.071 ± 0.006	0.097 ± 0.006
11 July[a]	0020	0042	2.34 ± 0.10	1.08 ± 0.06	0.06 ± 0.06		
11 July[a]	0216	0243	3.24 ± 0.09	1.15 ± 0.06	0.13 ± 0.05		
15 July	1752	1816	1.18 ± 0.14	0.89 ± 0.15			
20 July	1722	1739	2.53 ± 0.15	1.10 ± 0.07	0.04 ± 0.04		
21 July	1951	2009	3.18 ± 0.11	1.07 ± 0.05	0.16 ± 0.03		
22 July	1355	1424	2.36 ± 0.15	1.05 ± 0.08	0.24 ± 0.09		
22 July	1932	1940	3.3 ± 0.2	0.8 ± 0.2	0.2 ± 0.5		
25 July	1443	1455	2.3 ± 0.2	1.0 ± 0.2			
28 July	1540	1604	1.33 ± 0.10	0.85 ± 0.10		0.06 ± 0.04	
28 July	1642	1708	1.87 ± 0.04	1.22 ± 0.04	0.20 ± 0.02	0.024 ± 0.007	0.075 ± 0.011
			Enhancement Ratios, pptv ppbv^{-1}				
Other Studies			Acetonitrile	Benzene	Toluene	C_8-Aromatics	C_9-Aromatics
Utah			2.0	1.7	1.0	0.45	
Friedli[b]				1.35	1.325	0.6	
Andreae[c]			1.2	1.64	1.14	0.61	
Jost[d]			3.9	0.96	0.78	0.20	
Schauer[e]				1.28	0.45	0.25	
Holzinger[f]			1.3				
Sinha[g]				0.96	0.72		

[a]Flight departed on 11 July, but observations were made after midnight UTC on 12 July.
[b]Forest fire plumes in Montana [*Friedli et al.*, 2001].
[c]Literature survey, extratropical forest [*Andreae and Merlet*, 2001].
[d]Agricultural fires in Namibia [*Jost et al.*, 2003].
[e]Laboratory burning of pine [*Schauer et al.*, 2001] (using CO emission factor of 107 g kg^{-1}).
[f]Laboratory burning of savanna grasses [*Holzinger et al.*, 1999].
[g]African savanna fires [*Sinha et al.*, 2003].

described by both the GFS and ECMWF models, but since these layers were right above a pollution layer, the results were difficult to interpret and are not further examined in this paper. In all cases, FLEXPART underpredicted the observations.

[30] 6. Both the ECMWF and GFS models reproduced the position of the plume on 28 July very well (Figure 5h), largely independent of injection height. However, the FLEXPART model underestimated the measured acetonitrile by a factor 2–4. The ECMWF model with a 0–10 injection height predicted some features that were not observed by the aircraft.

[31] The grey areas in Figure 5 are the periods that are analyzed in detail in the following. They are also the periods for which the Δacetonitrile/ΔCO enhancement ratios were determined that are shown in Figure 4 and Table 2.

[32] Many of the fire plumes that were sampled by the NOAA WP-3 were best described using a 0–10 km injection height in FLEXPART, suggesting that these air masses were rapidly transported to high altitudes soon after emission. These findings are corroborated by the low humidity of the fire plumes. Figure 6 shows the altitude profiles of the dew point temperatures measured during the eight flights shown in Figure 3. The data points are color-coded by the measured mixing ratio of acetonitrile to show which parts of the flights were influenced by forest fire emissions. Almost all fire plumes had lower dew point temperatures than other air masses at the same altitude during the same flight. The exception is the flight of 22 July, when the fire-impacted air below 3 km had a higher dew point temperature than elsewhere during the flight. Even though the fire plumes were emitted at the surface, they were dryer than the surrounding air masses in the free troposphere. This suggests that the fire plumes had been processed by clouds and that moisture had been removed by precipitation. The dew point temperature in the fire plumes ranged from 0°C on 11 and 28 July, to −50°C on 15 July. These low values also suggest that some of the precipitation occurred at relatively high altitudes. Alternatively, the low dew point temperatures may be due to the mixing between the fire plumes and dry air at the northern latitudes where much of the transport took place. However, transport at northern latitudes was not exclusive to the observations of fires, and this may only partially explain the low dew point temperatures.

3.4. VOC Enhancements in the Fire Plumes

[33] Most of the VOCs measured from the aircraft were strongly enhanced in the fire plumes. An example is shown in Figure 7, which shows scatterplots of nine VOCs versus CO for the flight of 9 July. The data points are color-coded by the measured mixing ratio of acetonitrile to show which data were influenced by forest fire emissions. For acetaldehyde, MEK, toluene, and the C_8- and C_9-aromatics two groups of points can be seen. The black points at low acetonitrile mixing ratios were obtained early on in the flight on 9 July, when the outflow from Boston was sampled. The points at high acetonitrile mixing ratios were obtained in the fire plume, and it is seen that all of the VOCs were well correlated with CO. Enhancement ratios of all VOCs versus CO, ΔVOC/ΔCO, were determined by the slope of a line fitted by least squares regression to the data obtained in the fire plume. Enhancement ratios were calculated for all flights in Figure 3 (Tables 2 and 3). The data intervals used in the analysis are shown by the grey areas in Figure 5, and Tables 2 and 3 show the begin and end times

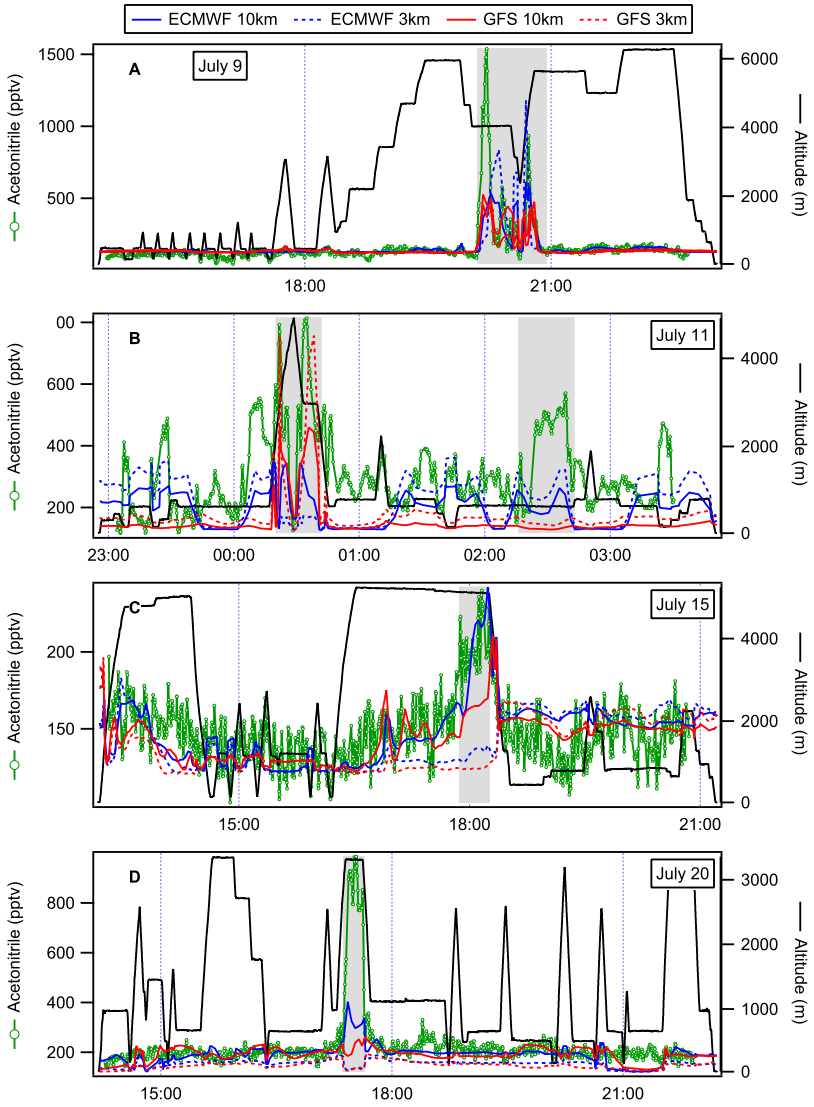

Figure 5. Measured acetonitrile data, in green, from (a) 9 July, (b) 11 July, (c) 15 July, (d) 20 July, (e) 21 July, (f) 22 July, (g) 25 July and (h) 28 July, along with the results from the FLEXPART model. The flight altitude is given in black.

of these episodes. In some cases, missing data (for toluene), the absence of a clear correlation between VOCs and CO, or VOC enhancements that were too small prevented the determination of meaningful VOC enhancement ratios, and no value is given in Tables 2 and 3. Finally, no enhancements in the plumes were observed for dimethyl sulfide, isoprene, methyl vinyl ketone, methacrolein and monoterpenes. On 11 and 28 July, when the fire plumes were observed in the boundary layer, there was some enhancement of biogenic species from regional sources.

[34] In 2002, the NOAA WP-3 sampled the outflow from a forest fire in Utah at close range [*de Gouw et al.*, 2003a]. It was estimated that the plume was intercepted two hours after its emission. *de Gouw et al.* [2003a] focused on the measurements of acetonitrile in the plume. In this paper, we have determined enhancement ratios for the other VOCs that were measured, and the results are added to Tables 2 and 3. No PTR-MS measurements were made of acetic acid, MEK and the C_9-aromatics in 2002, so those species are missing from Tables 2 and 3.

[35] The VOC enhancement ratios determined from all flights are plotted against the enhancement ratios of benzene in Figure 8. Benzene is chosen here, because it is strongly emitted from forest fires and had an atmospheric lifetime in these fire plumes that is comparable with the transport times. Different degrees of photochemical processing can therefore be inferred from the benzene enhancement ratios as will become apparent below. Each data point in Figure 8 shows the enhancement ratio determined from one plume crossing, and the flight dates are used to indicate the data points. Also added to Figure 8 are enhancement ratios from the Utah fire and emission ratios from the literature [*Andreae and Merlet*, 2001; *Friedli et al.*, 2001; *Schauer et al.*, 2001; *Jost et al.*, 2003; *Sinha et al.*, 2003]; the latter results are indicated by the name of the first author.

[36] Figure 8a shows the enhancement ratio of toluene versus the enhancement ratio of benzene. The toluene enhancement ratios are much lower, and the benzene enhancement ratios only slightly lower, than their respective emission ratios reported in the literature. The different

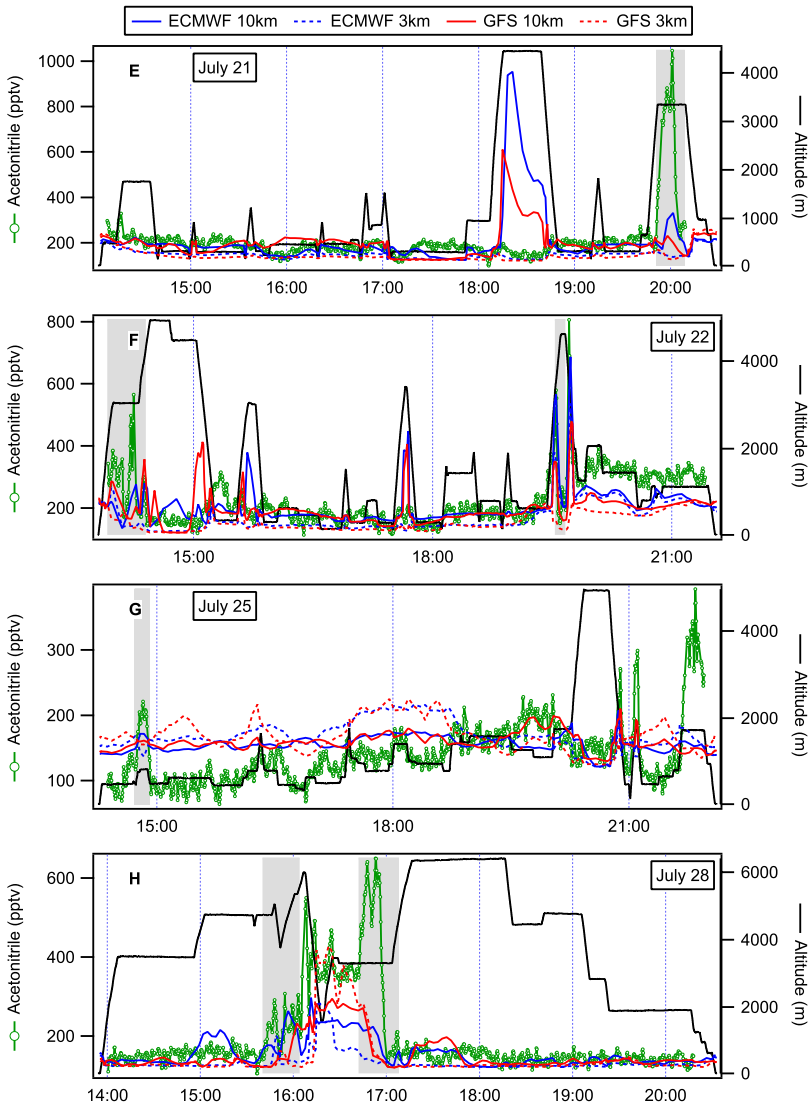

Figure 5. (continued)

behavior for toluene and benzene can be understood in terms of the chemical removal of these species: these VOCs are removed by OH in the atmosphere, and the reaction is more efficient for toluene (k = 5.63 × 10^{-12} cm^3 molecule^{-1} s^{-1}) than for benzene (k = 1.22 × 10^{-12} cm^3 molecule^{-1} s^{-1}) [*Atkinson and Arey*, 2003]. The emission ratio of *Jost et al.* [2003] and *Sinha et al.* [2003] do not seem to follow the general trend that is exhibited by the rest of the data. These data were obtained in the outflow from fires in Africa and may not be representative for North American forest fires.

[37] The enhancement ratios of toluene and benzene in the aged plumes can be described by:

$$\begin{aligned} \frac{\Delta\text{toluene}}{\Delta\text{CO}} &= \left.\frac{\Delta\text{toluene}}{\Delta\text{CO}}\right|_{t=0} \exp(-(k_{toluene} - k_{CO})[\text{OH}]\Delta t) \\ \frac{\Delta\text{benzene}}{\Delta\text{CO}} &= \left.\frac{\Delta\text{benzene}}{\Delta\text{CO}}\right|_{t=0} \exp(-(k_{benzene} - k_{CO})[\text{OH}]\Delta t) \end{aligned}, \quad (1)$$

where $\Delta\text{toluene}/\Delta\text{CO}|_{t=0}$ and $\Delta\text{benzene}/\Delta\text{CO}|_{t=0}$ are the emission ratios of toluene and benzene, and $k_{toluene}$, $k_{benzene}$ and k_{CO} are the rate coefficients for the OH reactions of toluene, benzene and CO. The parameter [OH] is the concentration of OH radicals, averaged over the transport time (Δt). The parameters [OH] and Δt can be eliminated from equations (1) to obtain [*McKeen et al.*, 1996]:

$$\left(\frac{\Delta\text{toluene}}{\Delta\text{CO}}\right) = \text{constant} \times \left(\frac{\Delta\text{benzene}}{\Delta\text{CO}}\right)^{\frac{k_{toluene}-k_{CO}}{k_{benzene}-k_{CO}}}, \quad (2)$$

where the constant is a function of $\Delta\text{toluene}/\Delta\text{CO}|_{t=0}$, $\Delta\text{benzene}/\Delta\text{CO}|_{t=0}$, $k_{toluene}$, $k_{benzene}$ and k_{CO}. It is assumed in equations (1) and (2) that there is no secondary formation of CO from VOC precursors. This assumption will be examined further below. Also, mixing between the forest fire plumes and background free tropospheric air can have a similar effect on toluene and benzene enhancement ratios as their chemical removal [*McKeen and Liu*, 1993; *McKeen et al.*, 1996]. It should be pointed out that that the fire plumes observed here consisted mostly of background air: CO in pure smoke can be as high as a percent, and had been reduced to less than 1 ppmv by the time the plumes were

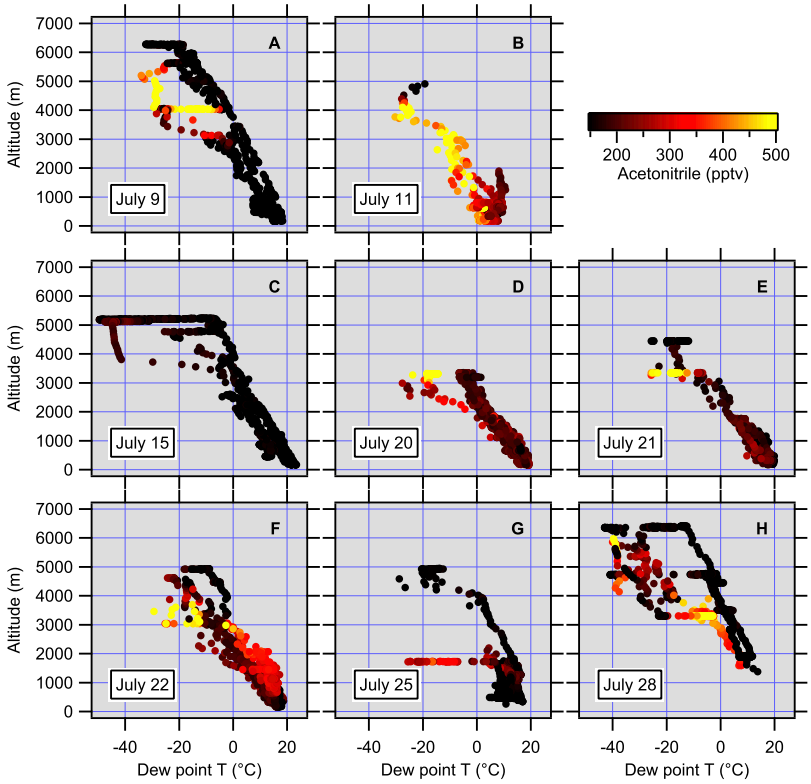

Figure 6. Altitude profiles of the dew point temperatures measured on (a) 9 July, (b) 11 July, (c) 15 July, (d) 20 July, (e) 21 July, (f) 22 July, (g) 25 July and (h) 28 July. The data points are color-coded by the measured acetonitrile mixing ratios.

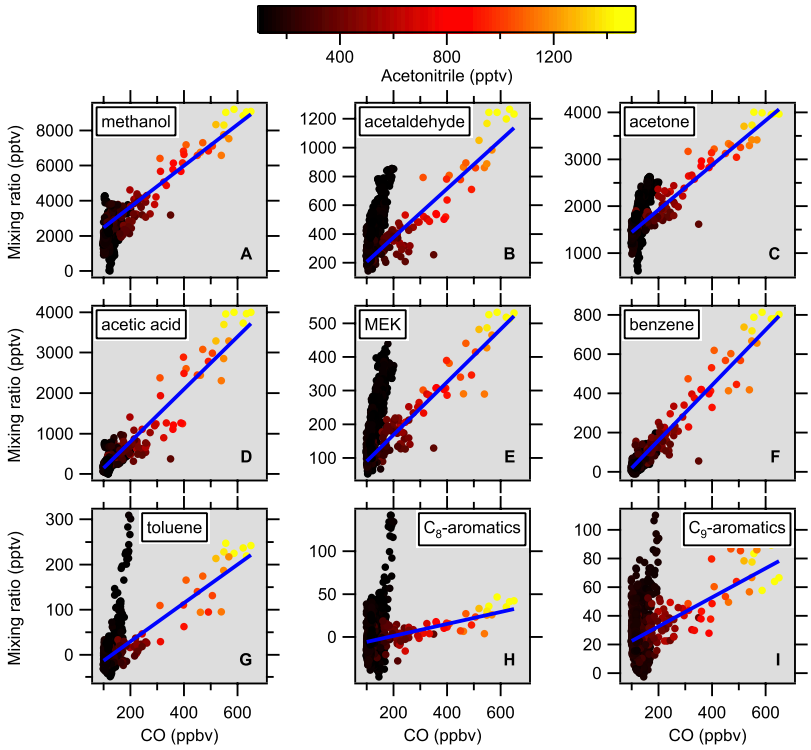

Figure 7. Determination of enhancement ratios for (a) methanol, (b) acetaldehyde, (c) acetone, (d) acetic acid, (e) MEK, (f) benzene, (g) toluene, (h) C_8-aromatics and (i) C_9-aromatics in the forest fire plume observed on 9 July 2004. The data are color-coded by the measured acetonitrile mixing ratio. The blue lines show the results of linear least squares fits to the data that were obtained during the plume intercept.

Table 3. Enhancement Ratios Relative to CO Determined for Five Oxygenated VOCs for the Different Forest Fire Plumes Sampled During NEAQS-ITCT 2k4

			Enhancement Ratios, pptv ppbv^{-1}				
Date	Start, UTC	Stop, UTC	Methanol	Acetaldehyde	Acetone	Acetic Acid	MEK
9 July	2006	2057	12.4 ± 0.5	1.68 ± 0.06	4.82 ± 0.11	6.4 ± 0.2	0.78 ± 0.02
11 July	0020	0042	10.2 ± 0.7	0.90 ± 0.07	4.5 ± 0.2	6.5 ± 0.4	
11 July	0216	0243	NC	0.40 ± 0.10	4.7 ± 0.2	1.2 ± 0.3	0.28 ± 0.04
15 July	1752	1816	21 ± 2	0.4 ± 0.4	7.9 ± 0.6	4.4 ± 0.8	0.5 ± 0.2
20 July	1722	1739	7.8 ± 0.4	1.17 ± 0.13	3.9 ± 0.2	6.6 ± 0.6	0.42 ± 0.06
21 July	1951	2009	5.4 ± 0.7	1.51 ± 0.11	3.8 ± 0.2	9.1 ± 0.5	0.56 ± 0.04
22 July	1355	1424	16 ± 2	1.3 ± 0.2	7.4 ± 0.7	7.4 ± 0.5	0.90 ± 0.11
22 July	1932	1940	9.6 ± 1.4		2.6 ± 0.3	0.9 ± 0.3	0.44 ± 0.13
25 July	1443	1455	2 ± 2	5.4 ± 0.5	22.8 ± 1.0	8.9 ± 0.9	1.9 ± 0.2
28 July	1540	1604	9 ± 2	1.3 ± 0.2	2.9 ± 1.0	5.7 ± 0.7	0.74 ± 0.11
28 July	1642	1708	14.9 ± 0.5	1.66 ± 0.05	3.68 ± 0.15	12.9 ± 0.5	0.73 ± 0.03
			Enhancement Ratios, pptv ppbv^{-1}				
Other Studies			Methanol	Acetaldehyde	Acetone	Acetic Acid	MEK
Utah			12.4	11.2	4.4		
Friedli[a]			2.4	2.7	2.05	0.42	2.6
Andreae[b]			16.4	2.85	2.50	16.6	1.65
Jost[c]					4.4		
Schauer[d]				10.1	3.38		0.78
Holzinger[e]			6.4	11.6	5.4		
Goode[f]			14			13	
Sinha[g]			15			16	

[a]Forest fire plumes in Montana [*Friedli et al.*, 2001].
[b]Literature survey, extratropical forest [*Andreae and Merlet*, 2001].
[c]Agricultural fires in Namibia [*Jost et al.*, 2003].
[d]Laboratory burning of pine [*Schauer et al.*, 2001] (using CO emission factor of 107 g kg^{-1}).
[e]Laboratory burning of savanna grasses [*Holzinger et al.*, 1999].
[f]Forest fire plumes in Alaska [*Goode et al.*, 2000].
[g]African savanna fires [*Sinha et al.*, 2003].

sampled. The effects of this mixing will also be discussed in the following.

[38] The shaded curves in Figure 8a show the result of fitting equation (2) to the data. Uncertainties in the individual data points (Table 2) were considered in the fit, but are not shown in Figure 8 for reasons of clarity. The solid curve in Figure 8a was obtained by setting the ratio $(k_{toluene} - k_{CO})/(k_{benzene} - k_{CO})$ at the value calculated from the rate coefficients (3rd column in Table 4). As the transport of the fire plumes generally took place at higher altitudes and latitudes, the use of room temperature rate coefficients may not be appropriate. We have calculated values for the ratio $(k_{toluene} - k_{CO})/(k_{benzene} - k_{CO})$ at 240 K using the temperature dependence of the rate coefficients given by *Atkinson and Arey* [2003] (4th column in Table 4). It is seen that the differences with the room temperature results are small except for acetic acid. The temperature dependence of the rate coefficients is thus a minor uncertainty in the analysis for all species but acetic acid. The dashed curve was obtained by fitting equation (2) to the data with the ratio $(k_{toluene} - k_{CO})/(k_{benzene} - k_{CO})$ a free parameter (5th column in Table 4). Data included in the fit are the measurements from NEAQS-ITCT 2k4, the Utah fire in 2002, and the emission ratios from the literature. Data from the African agricultural fires described by *Jost et al.* [2003] and *Sinha et al.* [2003] were not included, as they may not be representative of emissions from large boreal forest fires. The data from *Friedli et al.* [2001] also diverge from the general trend, but were included in the fit: these results were obtained in forest fires over Montana, which can be expected to be qualitatively similar to the fires studies in this paper. It is seen that the fitted curves in Figure 8a describe the data reasonably well. The best fit is obtained for $(k_{toluene} - k_{CO})/(k_{benzene} - k_{CO})$ equal to 3.5 ± 1.1, which is smaller than the value of 5.5 calculated from the literature values (Table 4). *McKeen et al.* [1996] performed similar analyses for hydrocarbon emissions in Asia, and also found smaller ratios of rate coefficients than expected from the OH kinetics. These differences were attributed to the mixing between the polluted outflow and the background free troposphere.

[39] The enhancement ratios for the other VOCs versus the enhancement ratio of benzene are shown in Figures 8b–8g. For species such as methanol and acetic acid the variability is high, suggesting that factors other than OH chemistry determine the enhancement ratios of these species. For example, it is possible that the emissions of these VOCs are more variable than the emissions of benzene and toluene. Emission factors typically depend on the type of fuel, and on the burning conditions (burning versus smoldering) [*Yokelson et al.*, 1997; *Goode et al.*, 2000]. Also, it is possible that nonchemical loss processes, such as removal by precipitation, affected the enhancement ratios of soluble VOCs more than those of aromatic VOCs. A discussion for each VOC follows:

[40] 1. Methanol emission ratios in the literature are highly variable (Table 3). The emission ratio given by *Friedli et al.* [2001] is much lower than those of *Andreae and Merlet* [2001], *Goode et al.* [2000] and the emission ratio observed in the Utah fire. However, the data from *Friedli et al.* [2001] were obtained using GC analyses of canister samples, which may not be reliable for methanol,

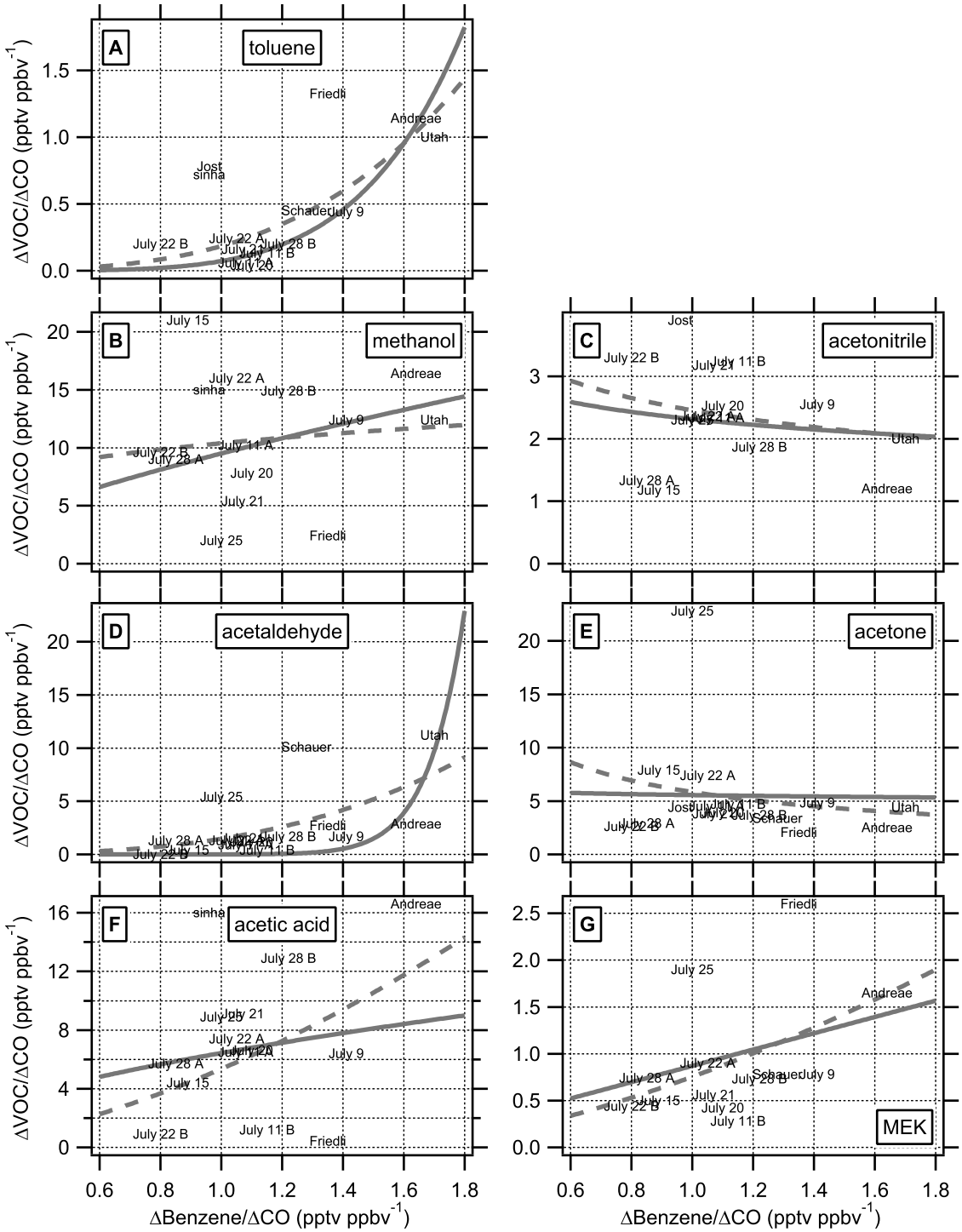

Figure 8. Observed VOC enhancement ratios versus CO, ΔVOC/ΔCO, as a function of the enhancement ratio of benzene versus CO, Δbenzene/ΔCO for (a) toluene, (b) methanol, (c) acetonitrile, (d) acetaldehyde, (e) acetone, (f) acetic acid and (g) MEK. The solid and dashed curves show the results of fitting equation (2) to the data with the parameter $(k_{toluene} - k_{CO})/(k_{benzene} - k_{CO})$ set at its literature value and determined by the fit, respectively.

and this could explain why the emission ratio is the lowest among all literature values listed in Table 3. During NEAQS-ITCT 2k4, highly variable methanol enhancement ratios were observed (Table 3 and Figure 8b). For example, on 25 July the methanol enhancement was nearly nonmeasurable, whereas on 15 July the enhancement was higher than any of the emission ratios cited in this paper. The shaded curves in Figure 8b show the results of fitting equation (2) to the data, and the fit results for the parameter $(k_{VOC} - k_{CO})/(k_{benzene} - k_{CO})$ are given in Table 4. Within the measurement uncertainties, there is no difference for methanol between the value of $(k_{VOC} - k_{CO})/(k_{benzene} -$

Table 4. Results of Fitting Equation (2) to the Scatterplots in Figure 8

VOC	OH Rate Coefficient,[a] cm^3 $molecule^{-1}$ s^{-1}	$(k_{VOC} - k_{CO})/(k_{benzene} - k_{CO})$[b]		
		At 298 K	At 240 K	From Fit
Toluene	5.63×10^{-12}	5.50	5.71	3.5 ± 1.1
Methanol	9.4×10^{-13}	0.71	0.58	0.2 ± 0.7
Acetonitrile	2.3×10^{-14}	−0.22	−0.29	−0.3 ± 0.5
Acetaldehyde	15×10^{-12}	15	24.8	3.1 ± 1.3
Acetone	1.7×10^{-13}	−0.07	−0.13	−0.8 ± 1.2
Acetic acid	7.4×10^{-13}[c]	0.51[c]	1.55[c]	1.7 ± 0.8
MEK	1.22×10^{-12}	1.00	1.18	1.6 ± 0.9

[a]At 298 K; *Atkinson and Arey* [2003].
[b]CO rate coefficient from *Sander et al.* [2002].
[c]*IUPAC Subcommittee on Gas Kinetic Data Evaluation for Atmospheric Chemistry* [2005].

k_{CO}) determined from the fit and from the published literature values. *Yokelson et al.* [2003] observed the wet removal of methanol in a fire plume, whereas *Holzinger et al.* [2005] inferred a secondary production of methanol in fire plumes from unusually high methanol enhancement ratios. The present data set does not contain systematic evidence for either effect, although it cannot be ruled out, of course, that the effects of cloud processing and secondary production canceled each other leading to a zero net change. *Lewis et al.* [2005] have shown that in anthropogenic pollution plumes the secondary production of methanol is mostly due to the oxidation of methane, which is not strongly emitted from biomass burning [*Brasseur et al.*, 1999]. In addition methane reacts much more slowly than the transport timescales of the sampled plumes. Because of the variability in the observed methanol enhancement ratio (Figure 8a), no firm conclusions can be drawn at this point.

[41] 2. For acetonitrile (Figure 8c), the enhancement ratio is approximately constant as the benzene enhancement ratio decreases, which is expected from the long atmospheric lifetime of acetonitrile. The fitted value of $(k_{VOC} - k_{CO})/(k_{benzene} - k_{CO})$ was very similar to the literature value (Table 4), and the fit results cannot be distinguished from the estimate from the literature in Figure 8c. If secondary production of CO had been significant, one would expect a decrease of the Δacetonitrile/ΔCO ratio as the benzene enhancement ratio decreases. This is not observed in the data outside of the experimental uncertainty.

[42] 3. For acetaldehyde, there is a large variability in the published emission ratios: the measured value of *Friedli et al.* [2001] and the literature survey of *Andreae and Merlet* [2001] are much lower than the results from *Holzinger et al.* [1999], *Schauer et al.* [2001] and our measurements in the Utah fire (Table 3). The measured enhancement ratios during NEAQS-ITCT 2k4 were lower than the average emission ratios in Table 3, consistent with the high reactivity of acetaldehyde. Fitting equation (2) to the data in Figure 8d resulted in a much lower value for the $(k_{VOC} - k_{CO})/(k_{benzene} - k_{CO})$ ratio than the literature value, whereas the value calculated for 240 K was even higher (Table 4). The effects of mixing could play a role, but the difference is larger than in the case of toluene. This suggests that secondary production of acetaldehyde may have been important. Secondary production of acetaldehyde is an important source in urban outflow [*de Gouw et al.*, 2005], so this is not surprising. On the other hand, some of the main precursors of acetaldehyde, short-chain alkanes and alkenes [*Lewis et al.*, 2005], are less prevalent in forest fire emissions [*de Gouw et al.*, 2004], and thus one can expect the secondary production of acetaldehyde to be less important in forest fire plumes than in urban plumes.

[43] 4. In the case of acetone, there is an obvious outlier in Figure 8e for the flight on 25 July. The other enhancement and emission ratios range from about 2–8 pptv $ppbv^{-1}$, but there is no obvious correlation with the enhancement ratio of benzene (Figure 8e). Acetone and CO have almost the same OH rate coefficient (Table 4), and thus the solid curve in Figure 8e is horizontal. The dashed curve with the fitted $(k_{VOC} - k_{CO})/(k_{benzene} - k_{CO})$ ratio shows a slight increase with decreased benzene enhancement ratios, which could be explained by secondary production as observed by *Jost et al.* [2003] and *Holzinger et al.* [2005]. However, the difference is not significant, and because of the variability in acetone enhancement ratios observed in this work no firm conclusions can be drawn regarding secondary production.

[44] 5. For acetic acid the emission ratio from *Friedli et al.* [2001] is much lower than the other two literature values given in Table 3, which may be explained by the loss of acetic acid in canister samples. The enhancement ratios of acetic acid observed in this work are all lower than the emission ratios from *Goode et al.* [2000] and *Andreae and Merlet* [2001]. Acetic acid is moderately reactive with OH ($k = 7.4 \times 10^{-13}$ cm^3 $molecule^{-1}$ s^{-1} [*IUPAC Subcommittee on Gas Kinetic Data Evaluation for Atmospheric Chemistry*, 2005]), so some decrease of acetic acid is expected as illustrated by the solid curve in Figure 8f. The dashed curve gives a steeper decrease of the acetic acid enhancement ratio, assuming the 298 K rate coefficient for acetic acid (Table 4). A recent IUPAC data evaluation, however, suggests that the temperature dependence of the acetic acid + OH reaction is strong [*IUPAC Subcommittee on Gas Kinetic Data Evaluation for Atmospheric Chemistry*, 2005], and the $(k_{VOC} - k_{CO})/(k_{benzene} - k_{CO})$ ratio derived from the data agrees well with the value calculated for 240 K (Table 4). No firm conclusions about secondary production or wet removal of acetic acid can be drawn from the data at this point.

[45] 6. As in the case of acetone, the MEK enhancement ratio on 25 July was far higher than the rest of the data points (Figure 8g). MEK has a similar OH reaction rate coefficient as benzene (Table 4), and a decrease of the MEK enhancement ratios with time is expected as illustrated by the solid curve. The difference between the values for $(k_{VOC} - k_{CO})/(k_{benzene} - k_{CO})$ from the fit and from the literature is insignificant (Table 4).

[46] The FLEXPART model can be used to estimate the transport times of the forest fire plumes that were sampled by the NOAA WP-3. Three examples are given in Figure 9, for the fire plumes observed on 9, 25 and 28 July. In all three cases there is not one single transport time, but rather a distribution of transport times with a width of several days. These widths are determined by a combination of factors. Each plume crossing sampled the emissions from fires in a large area, but even the emissions from a fire in one location would lead to an age spectrum with a width of several days because of different transport pathways in the atmosphere. The average transport times range from 4 ± 2 days for the plume on 28 July to 12 ± 2 days for 25 July. The latter value may be an underestimate, because the FLEXPART model

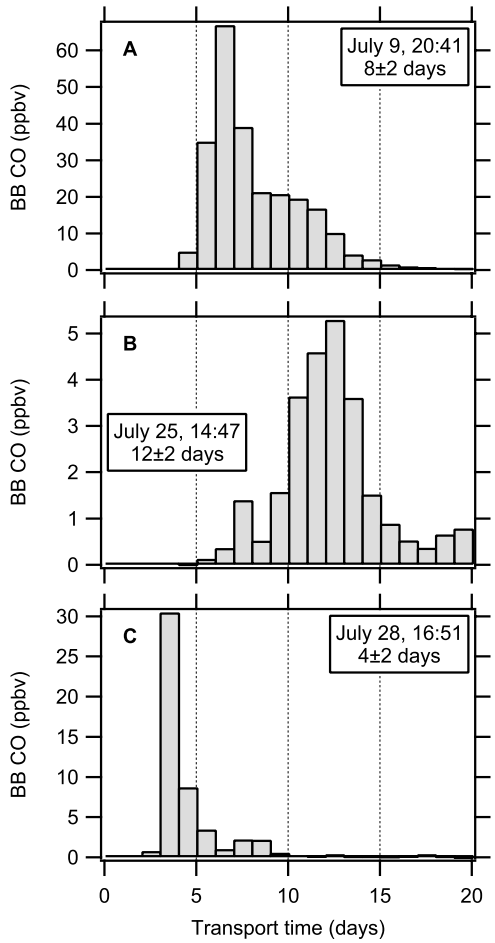

Figure 9. Examples of the distributions of transport times calculated using the FLEXPART model for forest fire plume intercepts on (a) 9 July, (b) 25 July and (c) 28 July.

only keeps track of the particle trajectories for 20 days. The shortest transport times were observed for the plume on 28 July, when there were fires further East in Canada and thus closer to the study area (Figure 2b).

[47] Figure 10 shows the enhancement ratios of benzene and toluene versus the average transport times from FLEXPART. There seems to be more scatter in Figure 10 than there was in Figure 8a. Chemically, the fire plume on 9 July seemed the least processed of all plumes observed (Figure 8a). However, the transport time was not particularly short (Figure 9a) and in the range of transport times for many of the other plumes. The plume on 25 July seemed one of the weaker and more processed plumes observed, and in agreement the average transport time according to FLEXPART was one the longest of all plumes. It should be noted that the degree of chemical processing of a fire plume not only depends on the transport time, but also on the photochemical history of the air mass. For example, did the emissions take place at night or during the day, were the emissions transported vertically in a fire-induced convective cloud, was humidity removed by precipitation, at what altitude and latitude did the plumes travel eastward, etc.

[48] The shaded curves in Figure 10 show the results of fitting equation (1) to the data. Uncertainties in the individual data points (Table 2) were considered in the fit, but are not shown in Figure 10 for reasons of clarity. Using the estimate of the transport time, Δt, from FLEXPART, the average concentration of OH radicals along the transport, [OH], can be calculated from the fit. An average OH concentration of $(4.4 \pm 0.9) \times 10^5$ molecules cm^{-3} is obtained from the benzene data in Figure 10a and $(4.5 \pm 1.3) \times 10^5$ molecules cm^{-3} from the toluene data in Figure 10b. The two values are in good agreement, but are much lower than the average OH concentrations that are expected at the average pressure altitude (500 hPa), latitude (52°N) and month of the year (July) of the transport. For example, from the OH climatology published by *Spivakovsky et al.* [2000] one would expect the average [OH] to be 1.75×10^6 molecules cm^{-3}, i.e., almost a factor of four higher. The exponential removal calculated using this OH concentration is shown by the dashed curves in Figures 10a and 10b, and it is seen that they do not describe the observed data well. Estimates of OH using the analysis shown in Figure 10 cannot be expected to be highly accurate (1) because of the mixing of the fire plumes with

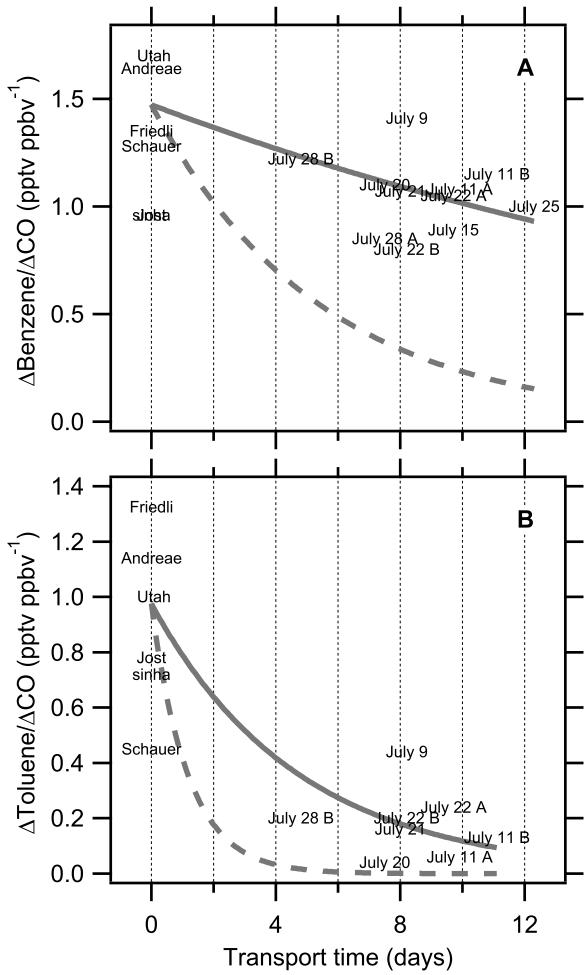

Figure 10. Enhancement ratios of (a) benzene and (b) toluene as a function of the transport times according to FLEXPART. The solid lines show the results of fitting equation (1) to the data with OH as a free parameter. The dashed lines show the result calculated using equation (1) and an OH concentration fixed at 1.75×10^6 molecules cm^{-3} according to an OH climatology.

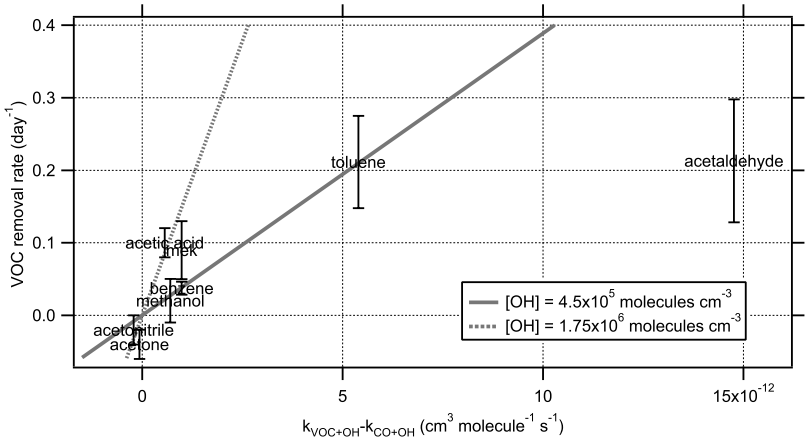

Figure 11. VOC removal rates in as a function of their rate coefficient for the reaction with OH.

background tropospheric air [*McKeen et al.*, 1996], (2) because of the mixing of fire plumes with different ages, and (3) because emission ratios from the literature played an important role in obtaining these results: Figures 8 and 10 show that the analysis presented here could not be done using the data from this study only but require emission ratios from the literature. Nevertheless, a difference of a factor of four between inferred and expected OH can probably not be accounted for by mixing. In addition, the observation of highly reactive species such as the C_8– and C_9–aromatics in the fire plume on 9 July (Figures 7h and 7i) after 8 days of transport (Figure 9a) strongly suggests that OH levels in the plume were indeed low: in an urban plume these compounds are typically removed within one day [*de Gouw et al.*, 2005], whereas *Hobbs et al.* [2003] observed a rapid removal of reactive VOCs in a fire plume in the first hour.

[49] OH is formed in the reaction between H_2O and O^1D atoms from ozone photolysis, and reacts efficiently with CO, methane and VOCs. A reduced OH in the fire plumes studied here can thus be expected because of the low humidity (Figure 6), the high levels of CO and other pollutants in the plumes, and to a lesser extent the reduction of photolysis rates [*Hobbs et al.*, 2003]. At the time of sampling the fire plumes generally did not contain large enhancements of NO_x and ozone, but did show increased levels of oxygenated VOCs such as acetone (Figure 7), which can provide an additional source of OH and HO_2 radicals [*Singh et al.*, 1995]. Preliminary box-model calculations, constrained by the observations, have indicated that 24-hour averaged OH concentrations in the fire plumes may have been as low as 5×10^5 molecules cm^{-3} in the most intense fire plumes (G. Chen, private communication, 2005). Also, *Forberich et al.* [1996] measured reduced levels of OH in a fire plume a few hours downwind from the source. In contrast with the present work, several studies have observed the removal of VOCs from fire plumes within hours [*Hobbs et al.*, 2003], and the question is why that did not happen in the plumes sampled here. We suggest that the rapid vertical transport of the emissions in fire-induced convection may have contributed to the inefficient removal of VOCs. As explained above, the presence of convective transport and the removal of water vapor by condensation and rainout are consistent with the observed low humidity of the plumes, as well as the fact that in many cases the fire emissions had to be injected above 3 km in FLEXPART to describe the data. During the convective transport, photolysis rates may have been severely depressed inside clouds, which significantly slows down the chemistry. Moreover, as a result of the convection, the fire emissions were transported to high altitudes where NOx is more efficiently stored as PAN (peroxyacyl nitrate), which is much more stable at low temperatures. Enhanced levels of PAN were indeed observed onboard the WP-3 in the fire plumes using a novel CIMS technique [*Flocke et al.*, 2004], but a detailed description of these measurements will be presented elsewhere. As described above, with NOx stored as PAN, the humidity low and CO high, a low OH can only be expected. At this point, the scenario outlined here is entirely speculative and needs to be verified, also quantitatively, by measurements closer to the outflow of fire-induced convection.

[50] Figure 11 shows the removal rates for all VOCs as a function of their rate coefficient for the reaction with OH. For benzene and toluene the removal rates were determined from the fits shown in Figure 10; similar analyses were made for the other VOCs included in Figure 11, but those are not shown here. Assuming that the loss is determined by reactions with OH, all data points should be on a straight line, the slope of which is equal to the average OH concentration. The solid shaded line is calculated using [OH] = 4.5×10^5 molecules cm^{-3}, determined from the removal of benzene and toluene, and the dashed curve using [OH] = 1.75×10^6 molecules cm^{-3}, expected from the OH climatology [*Spivakovsky et al.*, 2000]. It is seen that the dashed line does not describe the data well. The removal of acetaldehyde seems to be less than expected from the OH chemistry, which confirms the above conclusion that secondary formation of this compound was significant. The other VOCs follow the general trend relatively well. Acetic acid and MEK are slightly above the line, which suggests more efficient losses than expected from OH removal, possibly because of removal by precipitation. Acetone is slightly below the line, which could indicate secondary production. In all three cases, the uncertainty in the analysis is large and no firm conclusions can be drawn. We did not observe evidence for a large secondary formation source of methanol, acetone and acetic acid in the plumes as de-

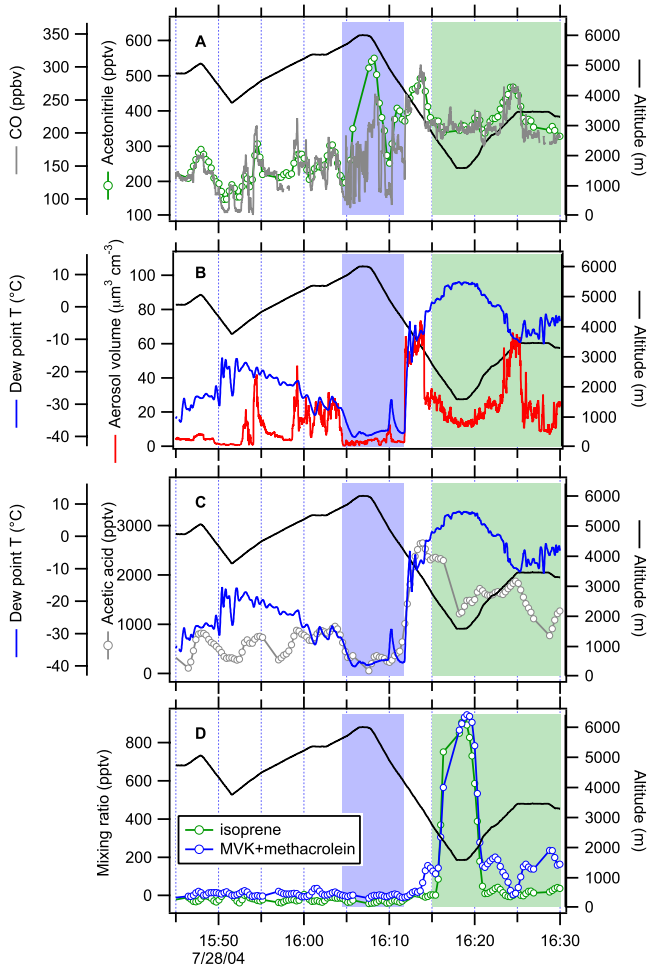

Figure 12. Results from the flight on 28 July for (a) acetonitrile and CO, (b) the aerosol volume and dew point temperature, (c) acetic acid and (d) isoprene and the sum of MVK and methacrolein. During the period marked in blue the aerosol volume and dew point temperature showed a marked decrease possibly due to precipitation scavenging.

scribed by several authors [*Mauzerall et al.*, 1998; *Goode et al.*, 2000; *Jost et al.*, 2003; *Yokelson et al.*, 2003; *Holzinger et al.*, 2005; *Trentmann et al.*, 2005]. Also, removal by cloud processing may not have removed methanol systematically from the plumes as observed by *Yokelson et al.* [2003] and *Tabazadeh et al.* [2004]. It may be possible that the effects of secondary production and cloud processing/precipitation removal partially canceled each other leading to the small net changes in oxygenated VOCs. The present data set with fire plume observations at least 4 days downwind from the sources do not allow very detailed conclusions about the VOC chemistry within the first few hours, such as discussed by *Jost et al.* [2003], *Yokelson et al.* [2003], *Hobbs et al.* [2003] and *Trentmann et al.* [2005].

3.5. Possible Observation of VOC Removal by Precipitation

[51] The measured volume concentration of submicron aerosol particles was in general well correlated with acetonitrile and CO in the fire plumes. An exception was observed during a brief interval on 28 July from 1605 to 1611 UTC, when both the particle volume and the dew point temperature decreased (period marked blue in Figure 12). Both acetonitrile and CO were substantially enhanced above their background mixing ratios during this interval, but did not show a similar decrease. The low dew point temperature of this air mass suggests that moisture might have been removed by precipitation. Interestingly, acetic acid, the most soluble VOC measured, also showed a minimum during the period marked in blue (Figure 12c). These observations suggest that particles and acetic acid had been removed from this air mass by precipitation scavenging.

[52] Between 1615 and 1630 UTC the NOAA WP-3 descended into the continental boundary layer and over 800 pptv of isoprene and MVK+methacrolein of biogenic origin were observed while the dew point temperature increased (Figure 12d). During this period (marked in green in Figure 12) acetonitrile and CO were both enhanced, indicating a substantial forest fire contribution within the boundary layer.

[53] Figure 13 shows scatterplots of the particle volume and VOC measurements versus CO for the entire period shown in Figure 12. The blue symbols represent the data collected during the period that may have been affected by precipitation scavenging (marked in blue in Figure 12), and the green points show data from the period in the boundary layer that was influenced by biogenic emissions (marked in green in Figure 12). The scatterplot of particle volume versus CO (Figure 13a) shows two very different groups of data points: the green and grey points follow a much steeper line than the blue points, which illustrates the low particle volume enhancement during the period that was possibly affected by precipitation scavenging. Of the VOCs measured, only acetic acid showed a substantial decrease in the enhancement ratio during the period of possible precipitation scavenging (Figure 13f). The other VOCs were not strongly affected by the possible precipitation (Figures 13b–13h): the blue points follow the same trend as the grey points. Interestingly, acetonitrile appears to be slightly enhanced during the period marked in blue, which may reflect variations in the source (Figures 12b and 13c).

[54] In the boundary layer acetonitrile and CO were well correlated (green points in Figure 13c), which indicates that the forest fire emissions were present down to the surface. Within the boundary layer, methanol, acetone, acetic acid and, less clearly, acetaldehyde and MEK were higher than expected from the average composition of the fire plumes: that is, the green points follow a steeper trend in Figure 13 than the blue and grey points. The additional contribution in these air masses most likely came from biogenic sources. *Karl et al.* [2003] quantified direct biogenic emissions of methanol, acetone and acetaldehyde, and secondary biogenic sources have been inferred from field data for acetic acid and MEK [*de Gouw et al.*, 2005].

4. Conclusion and Future Work

[55] In 2004 the NOAA WP-3 research aircraft intercepted merged, aged forest fire plumes from Alaska and western Canada during several flights of the NEAQS-ITCT 2k4 mission. Measurements of acetonitrile clearly proved that the air masses had been influenced by biomass burning. The location, altitude and timing of the plume crossings could be described well using emissions estimates and

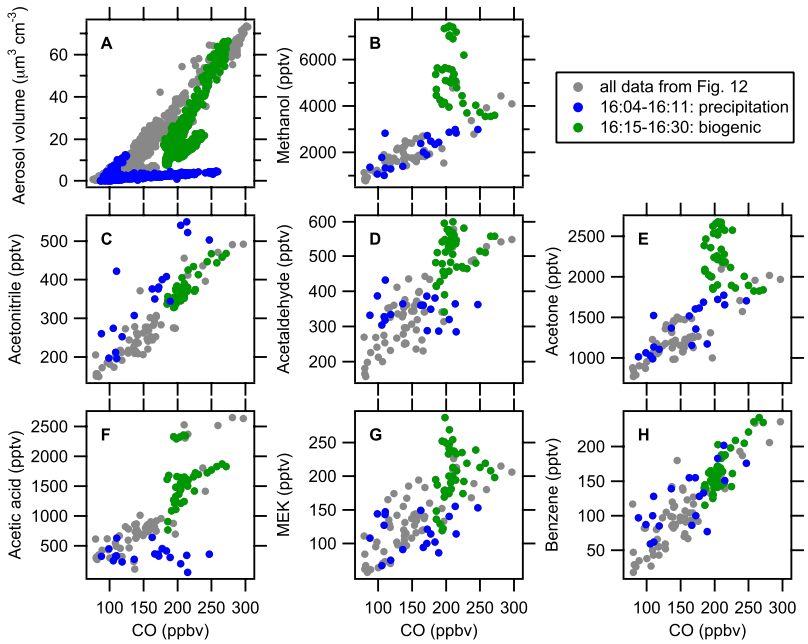

Figure 13. Scatterplots of (a) the aerosol volume, (b) methanol, (c) acetonitrile, (d) acetaldehyde, (e) acetone, (f) acetic acid, (g) MEK and (h) benzene versus CO for the measurement period of 28 July shown in Figure 12. The blue symbols show the data that were collected during the period that may have been affected by precipitation scavenging (marked in blue in Figure 12). The green symbols show data that were affected by biogenic emissions (marked in green in Figure 12).

calculations with the transport model FLEXPART. The best description of the data was often obtained when FLEXPART injected the forest fire emissions to high altitudes in the model. The observed plumes were generally drier than the surrounding air masses at the same altitude, suggesting that moisture may have been removed by cloud processing and precipitation. Different degrees of photochemical processing of the plumes were estimated from the measurements of aromatic VOCs. The removal of aromatic VOCs was slow considering the transport times estimated from the FLEXPART model. This suggests that the average OH levels were low during the transport, which may be explained by the low humidity, the lower photolysis rates and the high levels of CO and other pollutants. Secondary production of acetaldehyde was inferred from the measurements, but not for acetone, methanol and acetic acid, in contrast with previous work [*Mauzerall et al.*, 1998; *Goode et al.*, 2000; *Jost et al.*, 2003; *Yokelson et al.*, 2003; *Holzinger et al.*, 2005; *Trentmann et al.*, 2005]. A brief period with reduced enhancements of the measured particle volume was attributed to removal by precipitation. Of all VOCs measured only acetic acid was noticeably reduced during this period. Methanol was not reduced during this period, in contrast with the work of *Yokelson et al.* [2003] and *Tabazadeh et al.* [2004].

[56] Several details of the present study are intriguing, but may be difficult to explain with the available data. For example, the low humidity of the aged fire plumes suggests that the air masses had been processed by clouds and that moisture had been removed by precipitation. Nevertheless, particles and soluble trace gases were in most cases still present in the plumes, except during a brief period on 28 July. Because of the high variability of the VOC enhancements observed in the plumes and the high degree of dilution with background air, it was difficult to separate the effects of the variability in emissions, the secondary production of VOCs, and the scavenging by precipitation. It is hoped that future observations of forest fire emissions in the atmosphere can fill in some of these important open questions. Our conclusion that OH was relatively low seems more robust, and needs to be investigated further. If borne out by further research, these observations suggest that emissions from forest fires that were rapidly transported upward by fire-induced convection can be efficiently transported over thousands of kilometers without extensive chemical removal. If the fire plumes get mixed with the continental boundary layer, these reactive VOCs can participate in the VOC-NO_x chemistry and contribute to regional formation of ozone and organic aerosols.

[57] **Acknowledgments.** We thank the crew of the NOAA WP-3 and our NEAQS-ITCT 2004 collaborators. We thank the ECMWF for access to the meteorological data and N. Spichtinger for help with retrieving the data.

References

Andreae, M. O., and P. Merlet (2001), Emission of trace gases and aerosols from biomass burning, *Global Biogeochem. Cycles*, *15*, 955–966.

Atkinson, R., and J. Arey (2003), Atmospheric degradation of volatile organic compounds, *Chem. Rev.*, *103*, 4605–4638.

Bakwin, P. S., D. F. Hurst, P. P. Tans, and J. W. Elkins (1997), Anthropogenic sources of halocarbons, sulfur hexafluoride, carbon monoxide, and methane in the southeastern United States, *J. Geophys. Res.*, *102*, 15,915–15,926.

Brasseur, G. P., et al. (1999), Trace gas exchanges and biogeochemical cycles, in *Atmospheric Chemistry and Global Change*, edited by G. P. Brasseur, J. J. Orlando, and G. S. Tyndall, chap. 5, pp. 159–203, Oxford Univ. Press, New York.

Brock, C. A., et al. (2004), Particle characteristics following cloud-modified transport from Asia to North America, *J. Geophys. Res.*, *109*, D23S26, doi:10.1029/2003JD004198.

Christian, T. J., B. Kleiss, R. J. Yokelson, R. Holzinger, P. J. Crutzen, W. M. Hao, B. H. Saharjo, and D. E. Ward (2003), Comprehensive laboratory

measurements of biomass-burning emissions: 1. Emissions from Indonesian, African and other fuels, *J. Geophys. Res.*, *108*(D23), 4719, doi:10.1029/2003JD003704.

Christian, T. J., B. Kleiss, R. J. Yokelson, R. Holzinger, P. J. Crutzen, W. M. Hao, T. Shirai, and D. R. Blake (2004), Comprehensive laboratory measurements of biomass-burning emissions: 2. First intercomparison of open-path FTIR, PTR-MS, and GC-MS/FID/ECD, *J. Geophys. Res.*, *109*, D02311, doi:10.1029/2003JD003874.

Cofer, W. R., E. L. Winstead, B. J. Stocks, J. G. Goldammer, and D. R. Cahoon (1998), Crown fire emissions of CO_2, CO, H_2, CH_4 and TNMHC from a dense jack pine boreal forest fire, *Geophys. Res. Lett.*, *25*, 3919–3922.

DeBell, L. J., R. W. Talbot, J. E. Dibb, J. W. Munger, E. V. Fischer, and S. E. Frolking (2004), A major regional air pollution event in the northeastern United States caused by extensive forest fires in Quebec, Canada, *J. Geophys. Res.*, *109*, D19305, doi:10.1029/2004JD004840.

de Gouw, J. A., C. Warneke, D. D. Parrish, J. S. Holloway, M. Trainer, and F. C. Fehsenfeld (2003a), Emission sources and ocean uptake of acetonitrile (CH_3CN) in the atmosphere, *J. Geophys. Res.*, *108*(D11), 4329, doi:10.1029/2002JD002897.

de Gouw, J. A., C. Warneke, T. Karl, G. Eerdekens, C. van der Veen, and R. Fall (2003b), Sensitivity and specificity of atmospheric trace gas detection by proton-transfer-reaction mass spectrometry, *Int. J. Mass Spectrom.*, *223–224*, 365–382.

de Gouw, J. A., et al. (2003c), Validation of proton transfer reaction-mass spectrometry (PTR-MS) measurements of gas-phase organic compounds in the atmosphere during the New England Air Quality Study (NEAQS) in 2002, *J. Geophys. Res.*, *108*(D21), 4682, doi:10.1029/2003JD003863.

de Gouw, J. A., et al. (2004), Chemical composition of air masses transported from Asia to the U.S. West Coast during ITCT 2k2: Fossil fuel combustion versus biomass burning signatures, *J. Geophys. Res.*, *109*, D23S20, doi:10.1029/2003JD004202.

de Gouw, J. A., et al. (2005), The budget of organic carbon in a polluted atmosphere: Results from the New England Air Quality Study in 2002, *J. Geophys. Res.*, *110*, D16305, doi:10.1029/2004JD005623.

Flocke, F., et al. (2004), Fast time resolution airborne measurements of PANs during the New England Air Quality Study 2004 intensive, *Eos Trans. AGU*, *85*(47), Fall Meet. Suppl., Abstract A14A-01.

Forberich, O., J. Walter, and F. J. Comes (1996), Measurement of OH concentration during a forest fire episode: atmospheric implications for biomass burning, *Chem. Phys. Lett.*, *259*, 408–414.

Forster, C., et al. (2001), Transport of boreal forest fire emissions from Canada to Europe, *J. Geophys. Res.*, *106*, 22,887–22,906.

Friedli, H. R., E. Atlas, V. R. Stroud, L. Giovanni, T. Campos, and L. F. Radke (2001), Volatile organic trace gases emitted from North American wildfires, *Global Biogeochem. Cycles*, *15*, 435–452.

Goode, J. G., R. J. Yokelson, D. E. Ward, R. A. Susott, R. E. Babbitt, M. A. Davies, and W. M. Hao (2000), Measurements of excess O_3, CO_2, CO, CH_4, C_2H_4, C_2H_2, HCN, NO, NH_3, HCOOH, CH3COOH, HCHO, and CH_3OH in 1997 Alaskan biomass burning plumes by airborne Fourier transform infrared spectroscopy (AFTIR), *J. Geophys. Res.*, *105*, 22,147–22,166.

Hobbs, P. V., P. Sinha, R. J. Yokelson, T. J. Christian, D. R. Blake, S. Gao, T. W. Kirchstetter, T. Novakov, and P. Pilewskie (2003), Evolution of gases and particles from a savanna fire in South Africa, *J. Geophys. Res.*, *108*(D13), 8485, doi:10.1029/2002JD002352.

Holloway, J. S., R. O. Jakoubek, D. D. Parrish, C. Gerbig, A. Volz-Thomas, S. Schmitgen, A. Fried, B. Wert, B. Henry, and J. R. Drummond (2000), Airborne intercomparison of vacuum ultraviolet fluorescence and tunable diode laser absorption measurements of tropospheric carbon monoxide, *J. Geophys. Res.*, *105*, 24,251–24,262.

Holzinger, R., C. Warneke, A. Hansel, A. Jordan, W. Lindinger, D. H. Scharffe, G. Schade, and P. J. Crutzen (1999), Biomass burning as a source of formaldehyde, acetaldehyde, methanol, acetone, acetonitrile, and hydrogen cyanide, *Geophys. Res. Lett.*, *26*, 1161–1164.

Holzinger, R., J. Williams, G. Salisbury, T. Klupfel, M. de Reus, M. Traub, P. J. Crutzen, and J. Lelieveld (2005), Oxygenated compounds in aged biomass burning plumes over the eastern Mediterranean: Evidence for strong secondary production of methanol and acetone, *Atmos. Chem. Phys.*, *5*, 39–46.

IUPAC Subcommittee on Gas Kinetic Data Evaluation for Atmospheric Chemistry (2005), Summary of evaluated kinetic and photochemical data for atmospheric chemistry, edited by R. Atkinson et al., Research Triangle Park, N. C. (Available at http://www.iupac-kinetic.ch.cam.ac.uk)

Jost, C., J. Trentmann, D. Sprung, M. O. Andreae, J. B. McQuaid, and H. Barjat (2003), Trace gas chemistry in a young biomass burning plume over Namibia: Observations and model simulations, *J. Geophys. Res.*, *108*(D13), 8482, doi:10.1029/2002JD002431.

Karl, T., A. Guenther, C. Spirig, A. Hansel, and R. Fall (2003), Seasonal variation of biogenic VOC emissions above a mixed hardwood forest in northern Michigan, *Geophys. Res. Lett.*, *30*(23), 2186, doi:10.1029/2003GL018432.

Lavoué, D., C. Liousse, H. Cachier, B. J. Stocks, and J. G. Goldammer (2000), Modeling of carbonaceous particles emitted by boreal and temperate wildfires at northern latitudes, *J. Geophys. Res.*, *105*, 26,871–26,890.

Lewis, A. C., J. R. Hopkins, L. J. Carpenter, J. Stanton, K. A. Read, and M. J. Pilling (2005), Sources and sinks of acetone, methanol and acetaldehyde in North Atlantic air, *Atmos. Chem. Phys.*, *5*, 1963–1974.

Lobert, J. M., D. H. Scharffe, W. M. Hao, and P. J. Crutzen (1990), Importance of biomass burning in the atmospheric budgets of nitrogen-containing gases, *Nature*, *346*, 552–554.

Mauzerall, D. L., D. J. Jacob, S. M. Fan, J. D. Bradshaw, G. L. Gregory, G. W. Sachse, and D. R. Blake (1996), Origin of tropospheric ozone at remote high northern latitudes in summer, *J. Geophys. Res.*, *101*, 4175–4188.

Mauzerall, D. L., et al. (1998), Photochemistry in biomass burning plumes and implications for tropospheric ozone over the tropical South Atlantic, *J. Geophys. Res.*, *103*, 8401–8423.

McKeen, S. A., and S. C. Liu (1993), Hydrocarbon ratios and photochemical history of air masses, *Geophys. Res. Lett.*, *20*, 2363–2366.

McKeen, S. A., S. C. Liu, E. Y. Hsie, X. Lin, J. D. Bradshaw, S. Smyth, G. L. Gregory, and D. R. Blake (1996), Hydrocarbon ratios during PEM-WEST A: A model perspective, *J. Geophys. Res.*, *101*, 2087–2109.

McKeen, S. A., G. Wotawa, D. D. Parrish, J. S. Holloway, M. P. Buhr, G. Hübler, F. C. Fehsenfeld, and J. F. Meagher (2002), Ozone production from Canadian wildfires during June and July of 1995, *J. Geophys. Res.*, *107*(D14), 4192, doi:10.1029/2001JD000697.

Pfister, G., et al. (2005), Quantifying CO emissions from the 2004 Alaskan wildfires using MOPITT CO data, *Geophys. Res. Lett.*, *32*, L11809, doi:10.1029/2005GL022995.

Ryerson, T. B., et al. (2003), Effect of petrochemical industrial emissions of reactive alkenes and NO_x on tropospheric ozone formation in Houston, Texas, *J. Geophys. Res.*, *108*(D8), 4249, doi:10.1029/2002JD003070.

Sander, S. P., et al. (2002), Chemical kinetics and photochemical data for use in atmospheric studies, *Eval. 14*, *JPL Publ. 02-25*, Jet Propul. Lab., Pasadena, Calif.

Schauer, J. J., M. J. Kleeman, G. R. Cass, and B. R. T. Simoneit (2001), Measurement of emissions from air pollution sources. 3. C1–C29 organic compounds from fireplace combustion of wood, *Environ. Sci. Technol.*, *35*, 1716–1728.

Schauffler, S. M., E. L. Atlas, D. R. Blake, F. Flocke, R. A. Lueb, J. M. Lee-Taylor, V. Stroud, and W. Travnicek (1999), Distributions of brominated organic compounds in the troposphere and lower stratosphere, *J. Geophys. Res.*, *104*, 21,513–21,536.

Schauffler, S. M., E. L. Atlas, S. G. Donnelly, A. Andrews, S. A. Montzka, J. W. Elkins, D. F. Hurst, P. A. Romashkin, G. S. Dutton, and V. Stroud (2003), Chlorine budget and partitioning during the Stratospheric Aerosol and Gas Experiment (SAGE) III Ozone Loss and Validation Experiment (SOLVE), *J. Geophys. Res.*, *108*(D5), 4173, doi:10.1029/2001JD002040.

Singh, H. B., M. Kanakidou, P. J. Crutzen, and D. J. Jacob (1995), High concentrations and photochemical fate of oxygenated hydrocarbons in the global troposphere, *Nature*, *378*, 50–54.

Sinha, P., P. V. Hobbs, R. J. Yokelson, I. T. Bertschi, D. R. Blake, I. J. Simpson, S. Gao, T. W. Kirchstetter, and T. Novakov (2003), Emissions of trace gases and particles from savanna fires in southern Africa, *J. Geophys. Res.*, *108*(D13), 8487, doi:10.1029/2002JD002325.

Spivakovsky, C. M., et al. (2000), Three-dimensional climatological distribution of tropospheric OH: Update and evaluation, *J. Geophys. Res.*, *105*, 8931–8980.

Stohl, A., M. Hittenberger, and G. Wotawa (1998), Validation of the Lagrangian particle dispersion model FLEXPART against large scale tracer experiments, *Atmos. Environ.*, *24*, 4245–4264.

Stohl, A., C. Forster, S. Eckhardt, N. Spichtinger, H. Huntrieser, J. Heland, H. Schlager, S. Wilhelm, F. Arnold, and O. Cooper (2003), A backward modeling study of intercontinental pollution transport using aircraft measurements, *J. Geophys. Res.*, *108*(D12), 4370, doi:10.1029/2002JD002862.

Tabazadeh, A., R. J. Yokelson, H. B. Singh, P. V. Hobbs, J. H. Crawford, and L. T. Iraci (2004), Heterogeneous chemistry involving methanol in tropospheric clouds, *Geophys. Res. Lett.*, *31*, L06114, doi:10.1029/2003GL018775.

Trentmann, J., R. J. Yokelson, P. V. Hobbs, T. Winterrath, T. J. Christian, M. O. Andreae, and S. A. Mason (2005), An analysis of the chemical processes in the smoke plume from a savanna fire, *J. Geophys. Res.*, *110*, D12301, doi:10.1029/2004JD005628.

Warneke, C., J. A. de Gouw, W. C. Kuster, P. D. Goldan, and R. Fall (2003), Validation of atmospheric VOC measurements by proton-transfer-reaction mass spectrometry using a gas-chromatographic preseparation method, *Environ. Sci. Technol.*, *37*, 2494–2501.

Wofsy, S. C., et al. (1992), Atmospheric chemistry in the Arctic and sub-Arctic: Influence of natural fires, industrial pollution and stratospheric inputs, *J. Geophys. Res.*, *97*, 16,731–16,746.

Wotawa, G., and M. Trainer (2000), The influence of Canadian forest fires on pollutant concentrations in the United States, *Science*, *288*, 324–328.

Yokelson, R. J., D. W. T. Griffith, and D. E. Ward (1996), Open-path Fourier transform infrared studies of large-scale laboratory biomass fires, *J. Geophys. Res.*, *101*, 21,067–21,080.

Yokelson, R. J., D. E. Ward, R. A. Susott, J. Reardon, and D. W. T. Griffith (1997), Emissions from smoldering combustion of biomass measured by open-path Fourier transform infrared spectroscopy, *J. Geophys. Res.*, *102*, 18,865–18,878.

Yokelson, R. J., J. G. Goode, D. E. Ward, R. A. Susott, R. E. Babbitt, D. D. Wade, I. Bertschi, D. W. T. Griffith, and W. M. Hao (1999), Emissions of formaldehyde, acetic acid, methanol, and other trace gases from biomass fires in North Carolina measured by airborne Fourier transform infrared spectroscopy, *J. Geophys. Res.*, *104*, 30,109–30,126.

Yokelson, R. J., I. T. Bertschi, T. J. Christian, P. V. Hobbs, D. E. Ward, and W. M. Hao (2003), Trace gas measurements in nascent, aged, and cloud-processed smoke from African savanna fires by airborne Fourier transform infrared spectroscopy (AFTIR), *J. Geophys. Res.*, *108*(D13), 8478, doi:10.1029/2002JD002322.

E. L. Atlas, Rosenstiel School of Marine and Atmospheric Science, University of Miami, Miami, FL 33149, USA.

C. A. Brock, O. R. Cooper, J. A. de Gouw, F. C. Fehsenfeld, J. S. Holloway, M. Trainer, C. Warneke, and A. G. Wollny, NOAA Aeronomy Laboratory, Boulder, CO 80303, USA. (joost.degouw@noaa.gov)

S. G. Donnelly, Department of Chemistry, Fort Hays State University, Hays, KS 67601, USA.

A. Lueb and V. Stroud, National Center for Atmospheric Research, Boulder, CO, USA.

A. Stohl, Norwegian Institute for Air Research, Kjeller, Norway.